Warsaw University of Technology

Faculty of Electronics and Information Technology,

Institute of Electronic Systems

Daniel Jiménez Sánchez

Senior Design Project

IRIS SEGMENTATION AND NORMALIZATION METHODS FOR BIOMETRIC IDENTIFICATION

Project done under the supervision of

Dr inz. Zbigniew Wawrzyniak, PhD

Warsaw, June 2016

Abstract

Iris recognition systems capture an image from an individual's eye. The iris in the image is then segmented and normalized for feature extraction process. The performance of iris recognition systems highly depends on segmentation and normalization. For instance, even an effective feature extraction method would not be able to obtain useful information from an iris image that is not segmented or normalized properly. This thesis is to propose performance of segmentation and normalization processes in iris recognition systems to increase the overall accuracy.

The previous iris segmentation approaches assume that the boundary of pupil is a circle. However, according to our observation, circle cannot model this boundary accurately. Also, a warping method is developed due to off-axis orientations.

The results show the feasibility of the methods to work with occluded iris samples. It is found that the acquisition process is very important to improve an algorithm.

Contents

CHAPTER 1

Introduction

Personal identity is questioned frequently nowadays. Is a person authorized to access a certain resource? Is it this person who claims to be? Or even, who is this person? Throughout the technological development of mankind, several mechanisms were brought to life, locks and keys, secret passwords and PIN codes or key cards. Some of this technologies are more, some less secure. Although, all these mechanisms are need to be carried, in the case of keys, or need to be memorized, in the case of secret passwords. All these features can be shared and transferred between people, or just be lost.

Nowadays, the development of digital devices allows us to perform new methods to identify a specific person. This field of the science is called biometrics and use the body itself to recognise identities. To recognise a person we can use one or more characteristics of the human body, e.g. fingerprints, iris, ear structure, palm vein pattern, etc. Different characteristics give different biometric recognition performance and are differently accepted by the people.

No biometric system is free of error and it is always of interest to limit the error rates, so that the system performs better. It is internationally agreed by government, industry and academia that the performance of a biometric system is related to the quality of samples it work with. Indeed, poor quality samples can generate spurious or missing features which may lead to false rejections and false acceptances of genuine and impostor comparisons respectively.

Iris recognition is widely accepted as samples are fairly easy to collect. Algorithms developed for recognizing persons by their iris patterns have been tested in many field and laboratory trials, producing no false matches in several million comparison tests [1].

In 2001 the United Arab Emirates (UAE) Ministry of Interior launched a national border-crossing security programme using iris recognition. Nearly, 2 trillion (2 million-million) iris comparisons have been performed to date, as all foreign nationals visiting the Emirates have their irises compared against all the IrisCodes (mathematical descriptions of registered iris patterns) stored in a central database. The Abu Dhabi Directorate of Police report that so far there have been no False Matches [2].

If possible the sample can be manually assessed to ensure the best quality, e.g. during check-in, an airport officer inspects acquired iris samples. Should the quality be insufficient, sample

reacquisition may be necessary. Usually the subjects would be instructed how to behave and collaborate to have the best acquisition quality.

Measuring the quality allows to decrease error rates of biometrics systems by rejecting poor quality samples, yet no feedback is provided to the use on why the quality is poor. If a sample is reacquired with unchanged conditions, the quality may remain the same. That condition could be the uncontrolled light in the environment or unexpected elements on the region of the iris. Anyway, the development of algorithms improves the processing of poor quality images. It is interesting to check whether these samples indeed cause performance degradation and if so, if it is possible to automatically distinguish them and provide accurate feedback.

CHAPTER 2

Biometrics

This chapter gives an overview of biometrics systems. The general concept of biometrics recognition is introduced; performance and errors of a biometric system are discussed. Finally, biometric iris recognition is described.

The concepts are illustrated accordingly to the ISO/IEC 29794-1 standard [3] developed by International Electro technical Commission of International Organization for Standardization (ISO/IEC). Vocabulary is used accordingly to the ISO/IEC JTC 1/SC 37 Harmonized Biometric Vocabulary defined in SC37 Working Group 1 for the International Standard ISO/IEC 2382-37 [4].

2.1 Introduction

The word *Biometrics* comes from Greek *bios* (life) and *metron* (measurement). Biometric identifiers are anatomical and behavioural characteristics (traits) of a human body.

Nowadays, the standard definition of biometrics is 'the process by which a person's unique physical and other traits are detected and recorded by an electronic device or system as a means of confirming identity'

2.2 Biometric modality

Theoretically, any trait or body characteristic (also called modality) could be used in biometrics as long as it is:

- *Universal* – every person has it,
- *Distinctive* – no two people have it identical,
- *Permanent* – unchanged over time,
- *Collectible* – it can be measured quantitatively.

In practice, a biometric trait is also evaluated based on the performance it gives in terms of speed, recognition accuracy and ease of circumvention. It is also important to assess how capturing a certain characteristic is accepted by people, e.g. some people may prefer not to have their faces recorded.

Several characteristics are used in biometrics successfully, some examples of modalities are:

- Iris – using iris visual texture,
- Fingerprint – using ridge line structure,
- Face – using facial features size and distance,
- Vein – analysing the vein structure of the palm or finger,
- Voice – measuring the sound characteristics of speech.

2.3 Biometric terminology

Certain terminology has very specific meaning in the context of biometrics. The process of obtaining a biometric sample is *acquisition*. Samples are captured and turned into digital signatures using a *sensor*. *Enrolling* is the process of acquiring a biometric sample, along with other information, to be used as part of the database. The process of comparing a probe sample and database sample is called *matching*, which returns a *match score*. Samples are compared using one of many *algorithms*. A biometrics system usually has a *threshold* value, which determines whether the match score indicates a *match* (meaning that the samples are likely of the same person) or a *non-match* (meaning that the samples are probably of two different people).

2.4 Biometric processes

Biometric recognition can be applied in several contexts, e.g. granting or denying access, confirming claimed identity or simply for identity recognition. However, all systems have several elements in common – all systems capture and store the data, perform signal processing, comparing and make biometric decisions.

Figure 2.1 shows a diagram of a conceptual biometric system structure with the common elements grouped. This process is generally performed as follows:

1. Data Capture: biometric sensor acquires a sample from a subject,
2. Processing : the sample is analysed and features extracted,
3. Enrolment Template: the resulted features can be saved in the database as a biometric reference, or compared with one or more existing templates during verification or identification.
4. Comparison: determines the comparison score between captured sample and stored reference,
5. Match: is made based on the comparison scores.

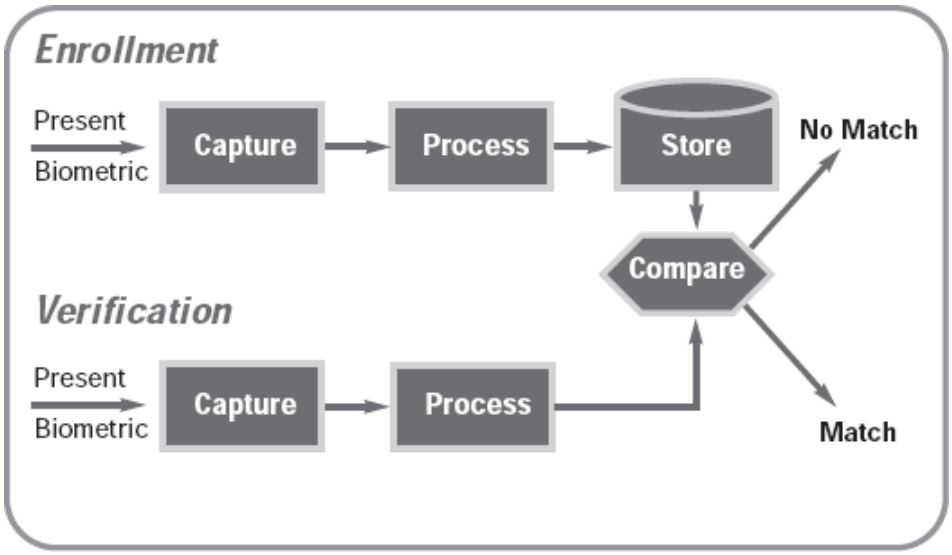

Figure 2.1: The process of enrolment and authentication

2.5 Biometric comparison

The one-to-one comparison of verification is the process of calculating the similarity or dissimilarity between two biometric samples – the probe and the reference. If a biometric comparison is done between two samples that are taken from the same characteristic of the same person, it is a mated comparison. Otherwise, the comparison is non-mated. ISO/IEC 2382-37 defines this as follows:

- Mated: "a comparison of a paired probe and reference from the same characteristic of the same data subject" [5]
- Non-mated: "a comparison of a probe and a reference from the same characteristic of different data subjects"

2.6 Biometric decision

The *comparison score* is used to give the *comparison decision* based on whether the score is above or below a certain threshold as follows:

- *Match*: score above the threshold gives a positive comparison decision "stating that the biometric probe and the biometric reference are from the same source"
- Non-match: score below the threshold gives a negative comparison decision "stating that the biometric probe and the biometric reference are not from the same source"

2.6 Biometric system errors

Even though biometric systems use sophisticated hardware and state of the art algorithms, sometimes errors are inevitable. A comparison decision is not always correct, sometimes mated samples are rejected and non-mated accepted, which results in the following errors:

- False Rejection: biometric decision of a non-match from a comparison of mated samples. Defined as "error of rejecting a biometric claim that should have been accepted in accordance with an authoritative statement on the origin of the biometric probe and the biometric reference"
- False Acceptance: biometric decision of a match from a comparison of non-mated samples. Defined as "error of accepting a biometric claim that should have been rejected in accordance with an authoritative statement on the origin of the biometric probe and the biometric reference"

Errors of biometric systems that were not caused during the comparison procedure are also specified, as defined by ISO/IEC 2382-37.

- Fail To Capture (FTC): the capturing module may fail to properly capture the sample.
- Fail To Process (FTP): the feature extraction module may fail to process a sample.
- Fail To Acquire (FTA): a combination of three first errors – FDC, FTC, FTP – a general failure in sample acquisition.
- Fail To Enrol (FTE): the template generation module can fail to extract a template resulting in an enrolment failure.

2.7 Iris Recognition Systems

Biometric iris recognition systems use the anatomical characteristic of a person's iris pattern. The iris consists of two layers; the front pigmented fibrovascular known as a stroma and, beneath the stroma, pigmented epithelial cells. An iris-recognition algorithm can identify up to 200 identification points including rings, furrows and freckles within the iris. Figure 2.2 shows examples of iris samples acquired using different sensors.

(a) (b) (c)

Figure 2.2 Iris samples acquired using different scanners. a) circular NIR LED array illumination b)Irispass-h [6] c) NIR acquisition.

In a 1953 clinical textbook, F.H. Adler wrote: *"In fact, the markings of the iris are so distinctive that it has been proposed to use photographs as a means of identification, instead of fingerprints".* With the development of camera devices, some iris recognition systems had been developed.

There are two types of acquiring systems, near infrared (NIR) and visible wavelength (VW) imaging. Those systems acquire different information of the iris. Visible light reveals rich pigmentation details of an iris by exciting the melanin, and near infrared spectrum enables the blocking of corneal specular reflections from a bright ambient environment. Figure 2.3 shows examples of iris samples in NIR and VW spectrum.

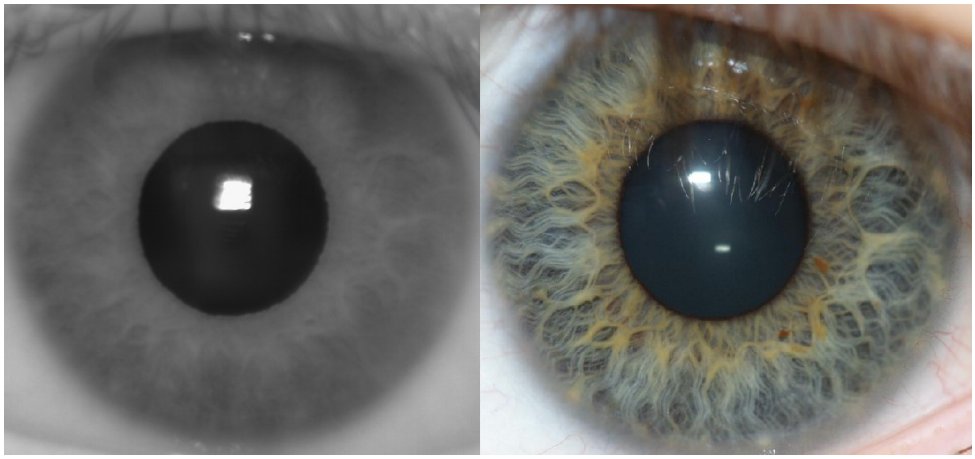

(a) (b)

Figure 2.3 Iris samples acquired using different spectrums a) NIR b) VW

2.8 Iris Sample Acquisition

In order to obtain a good iris sample, we must take into account the situation of the acquisition. Is somebody supervising the acquisition of the image? Where is the image acquired? What are the characteristics of the subject's eye? Those questions should be asked in order to make a correct algorithm.

The state of the art comes up with the idea of introducing the iris recognition identification into the smartphones. Worldwide universities and companies are looking for solutions. Some researchers from the Warsaw University of Technology [7] explored the feasibility of iris recognition for visible spectrum iris images obtained using smartphone camera. Some of the images obtained by the researchers are shown in Figure 2.4.

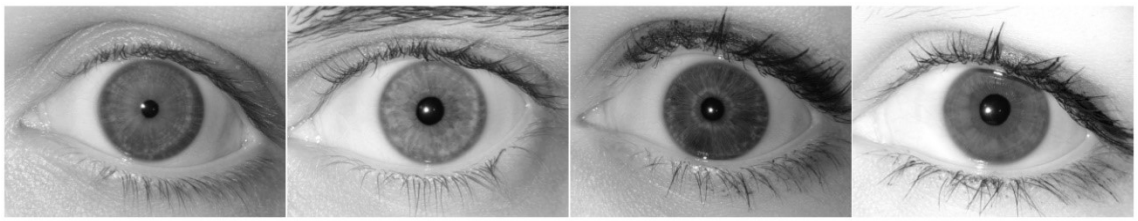

Figure 2.4: Grayscale images of the smartphone database

Those images are from different types of eyes, lightly pigmented irises, blue-green and hazel-green. The iris tissue pattern is easily discernible in each sample, because the eye is wide open and the contrast of the acquisition is good. But, in a future approach, the subjects would have the eye less opened due to its position. If the subject takes the mobile device with his hand, the eye wouldn't be looking to the camera. Instead of that, the eye would be looking to the screen of the smartphone, which is below the camera.

In an approach to look for a real situation, this work uses a different database. The OKI IRISPASS-h database uses a hand-held device to obtain the images. This hand-held device looks like a smartphone, as shown in Figure. 2.5. [6] [8]

Figure 2.5: The hand-held iris camera OKI IRISPASS-h

CASIA database was used for first time in the 5th Chinese Conference on Biometrics Recognition (Sinobiometrics 2004), held in GuangZhou, China in December 2004. The device was developed by OKI, and the images obtained by the Chinese Academy of Sciences. Some statistics and features are summarized on figure 2.6.

Subset / Characteristics	device1
Sensor	OKI IRISPASS-h
Environment	Indoor
Session	one
No. of classes	60
No. of images	1200
Resolution	640*480

Figure 2.6: Statistics of CASIA Iris Image database.

In the chapter 3 we will talk about the image quality of the database because, the aim of this chapter is just to explain why is interesting to use this database. In Figure 2.7 we can see some images from the database, and we can check the typology of the eyes of the subjects. The subjects of the database are from China, and it is known that the Asian eyes are different to other human races. So, the eyes are not so open and we can't see all iris pattern.

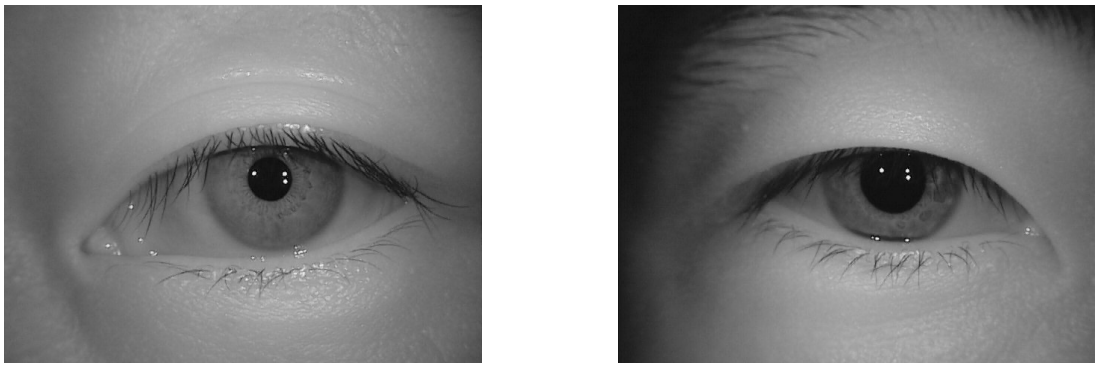

Figure 2.7: Images of the CASIA database.

CHAPTER 3

Biometric Sample Quality

This chapter discusses the biometric sample quality. First the concept is introduced, secondly the uses of quality measure are discussed with possible applications. Finally, the quality of iris samples is described and related to the earlier introduced concepts.

3.1 Introduction

Biometric sample quality is a measure of the usefulness of a biometric image. The researchers are interested in standards for measurement of biometric quality. For example, ISO has established a biometric sample quality draft standard [9]. According to ISO standard, biometric sample quality may be considered from the point of view of character (inherent features), fidelity (accuracy of features), or utility (predicted biometrics performance). A general consensus has developed that the most important measure of a quality metric is its utility – images evaluated as higher quality must be those that result in better identification of individuals, as measured by an increased separation of genuine and impostor match score distributions.

The term quality should not be solely attributable to the acquisition settings of the sample, such as image resolution, dimensions in pixels, greyscale bit depth, illumination of the image, or contrast of the environment. Though such factors may affect sample utility and could contribute to the overall quality score.

3.2 Quality Purpose

The information about sample quality can be applied in several ways in biometric systems. Quality can be assessed on-line after sample acquisition and utilised immediately, or computed off-line on an existing set of earlier acquired samples.

Output of different quality metrics can be combined together in various manners, since using the same quality metrics in different applications is challenging - as described earlier, different systems may benefit from utilising different quality information [10].

Quality algorithms shall produce quality scores that predict performance metrics such as either false match or false non-match. In cases where the system utilizes components from multiple vendors, the quality scoring methods should aim to reflect the aspects of performance important for each algorithm used.

3.2 Survey and Diagnosis

Quality information may be extracted from samples which had previously been captured. This is useful for survey statistics where scores from e.g. different operational sites are analysed to identify trends or anomalies in performance.

Another use of off-line quality information is correlation between different system metrics. This may help to improve the acquisition procedure and is useful in order to give a full overview of the system quality.

The diagnosis of the quality is also related to the external conditions. Who is taking the image? How is he controlling the acquisition procedure? Where is taking place the image? In fact, the quality of the image depends more on the external features of the environment than in the internal.

3.3 Iris Pattern sample quality

Iris recognition systems use the iris pattern features as the biometric characteristic. Two Iris patterns are never identical [11], the captured image depends highly on several factors such as:

- Iris acquisition
    - Dedicated illumination
    - Defocus
    - Dynamic range
    - Motion blur
    - Noise (or camera sensitivity)
    - Occlusion due to specular reflections
    - Optical distortion
    - Optical resolution
    - Pixel aspect ration
    - Pixel sampling
- Iris subject
    - Deviation from circularity in iris-sclera border and iris-pupil border
    - Eye colour
    - Eye wear

- Intrinsic iris-pupil contrast
- Intrinsic iris-sclera contrast
- Occlusion due to eyelash/eyelid
- Off-axis Orientation – head rotation
- Off-axis Orientation – sight direction
- Pupil size

Those factors complicate or enable the Iris recognition system. There are two types of factors, the related to acquisition and the related to the subject. The researchers have to focus on the acquisition factors because we can't improve the factors involving the subjects. During the development of cameras new solutions were shown and it's known that the illumination is one of the most important factors can be enhanced.

The iris subject factors may be considered on the development of the algorithm. Do the iris features change depending on these factors? Can we solve these issues by improving the method? The acquired image is just a projection of the real eye, so the algorithm should match different projections of the same eye.

The off-axis orientation due to the sight direction changes the dimensions by warping the iris features. In Fig. 3.1 it's shown the off-axis orientation, the iris pattern is the same in both images but the camera acquires different projections of the eye.

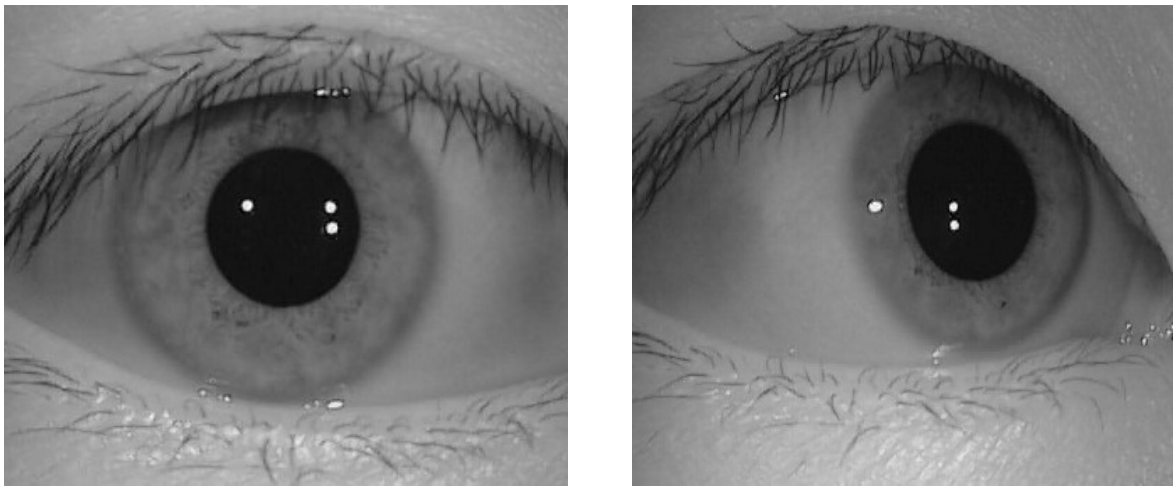

Figure 3.1: The off-axis orientation due to sight direction changes.

The change of pupil size due to alterations in illumination is an important factor to consider. It modifies the size of the iris pattern and changes its definition. In order to control the size of the pupil some acquisition systems include illumination. Anyway, the pupil size depends on the illumination of the environment, and we can't control it. In Fig. 3.2. its shown the different pupil sizes with illumination.

In the first moment, we can say that a bigger pupil of the same person may cover part of the iris pattern. But that's not true, the iris surface warps into other dimensions in order to let the pupil have the necessary size.

Figure 3.2: Eyes with different pupil size

In chapter 2, we talked about iris recognition on hand-held devices such as smartphones. In a real situation which the subject is looking into the screen of the smartphone, there is a occlussion due to eyelash and eyelid. In the CASIA database there's occlusion, and we explained why its important to study these kind of images. In figure 3.3, its shown different kind of occlussions. The most common occlusion its upside the pupil, but if the subject is looking down there is a occlussion besides the pupil.

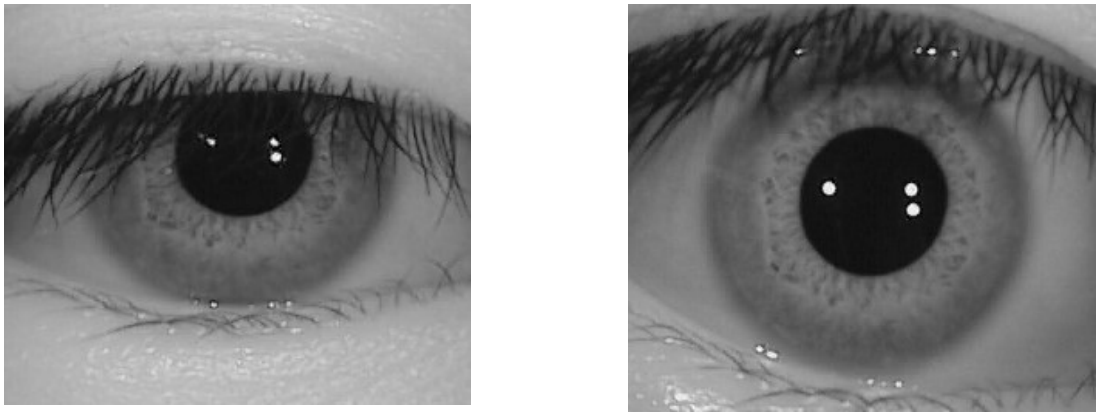

Fig. 3.3: Example of eyelid and eyelash occlusion.

CHAPTER 4

State of the art in iris recognition methods

This chapter describes the state of the art algorithm for iris recognition systems. Several methods for iris segmentation exist. [1] [7] [12] [13]

4.1 Introduction

Algorithms developed by authors for recognizing persons by their iris pattern have been tested in many field and laboratory trials, producing no false matches in several million comparison tests. John Daugman's work in the field is well known, and his algorithms were tested and patented. Here is discussed the John Daugman's methods for iris recognition. Those algorithms were presented and explained in several articles and papers. Also, other author's algorithms for iris segmentation are discussed.

4.2 How Iris Recognition works

Every iris recognition algorithm has 4 main steps; iris segmentation, iris normalization, iris template creation and iris template comparison. To capture the rich details of iris patterns, an imaging system should resolve a minimum area of iris pattern, in order to give precise information to the system. Typically, acquisition systems take (480x640) images and about 10% of the image is iris pattern.

4.2.1 Iris Segmentation

There exist many alternative methods for finding and tracking facial features such as the eyes. The iris segmentation is one of the most important steps in iris recognition, because the system works with segmented iris. If the iris segmentation fails, the entire procedure is pointless. Basically, different algorithms they differ in the iris segmentation procedure. We

have to say that different techniques should be used to different databases. Moreover, the image processing changes depending on the used sensor. For these reasons, the iris segmentation method is not unique. One method is shown below.

Iris recognition begins with demarcating the iris inner and outer boundaries at the pupil and sclera, detecting the upper and lower eyelid boundaries if they occlude, and detecting and excluding any superimposed eyelashes or reflections from the cornea or eyeglasses. We call these processes iris segmentation. [13] It is natural to start by thinking of the iris as an annulus. Soon, one discovers that the inner and outer boundaries are not concentric. And one also discovers that, often, the pupil boundary is not circular. John Daugman's method uses active contour, because they allow for noncircular boundaries. In the case of the outer boundary, it is often partly occluded by eyelids so that the boundary is noncircular.

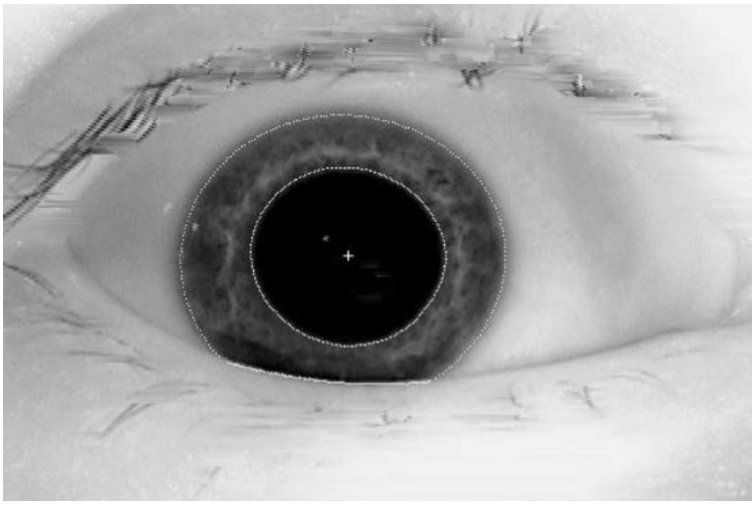

Figure 4.1: Iris inner and outer boundaries using active contour

Active contour is shape model that deforms a desired contour (a circle) to energy minimized 'snake'. Given an initial guess for a snake, the energy function of the snake is iteratively minimized. The energy formulation is given by employing discrete Fourier series expansions of the contour data. Selecting the number of frequency components allows control over the degree of smoothness that is imposed. On figure 4.1 two 'snakes' are illustrated, one for the pupil and other for the iris.

The interruptions correspond to detected occlusions by an eyelid, which is indicated by separated line in image. As it has been said, active contour uses a guessed contour to calculate the 'snake' so that the approximated circle is important to the success or fail of the method.

A limitation of current iris recognition cameras is that they require an on-axis image of an eye, which is usually achieved by the user aligning his optical axis with the camera´s optical axis. Anyway, some images in the database don't have an on-axis image of an eye. In order to solve this problem, John Daugman developed a solution by correcting the projective deformation of the iris when it is imaged off-axis, provided that one can estimate how the iris is deformed. A projective transformation is improved with the information of the pupil boundary, if the

'snake' is an ellipse a projective deformation is done with the purpose of obtaining a circular pupil.

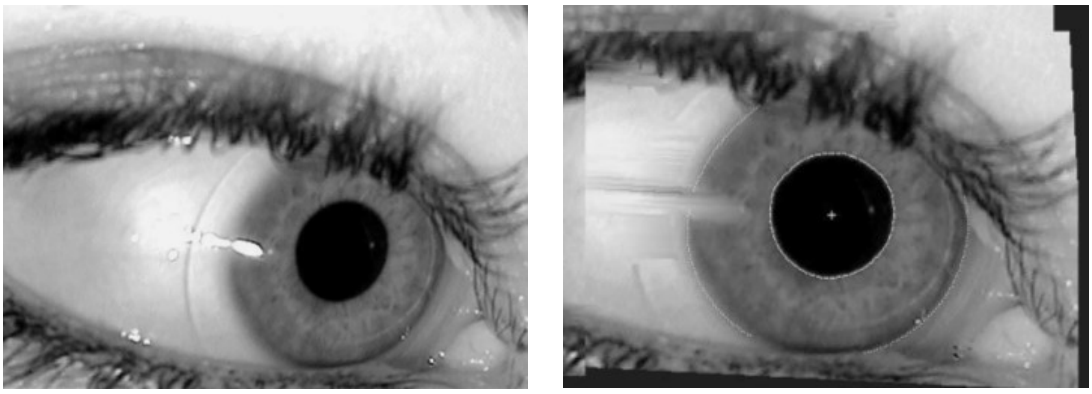

Figure 4.2: From left to right, the original image and the projective deformed.

4.2.2 Iris Normalization

A normalization is needed because the system compares two iris Images. A normalized iris is an image with a specific size and resolution. John Daugman devised a homogeneous rubber sheet model remapping each point within the iris region to a pair of polar coordinates (r, θ) where r is on interval [0,1] and θ is angle [0, 2π].

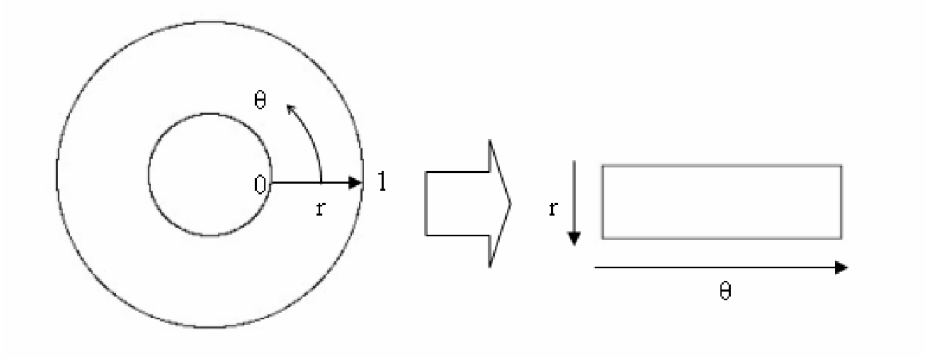

Figure 4.3: Daugman's rubber sheet model

The remapping of the iris region from (x,y) Cartesian coordinates to the normalised non-concentric polar representation is modelled as

$$I\big(x(\mathrm{r},\theta),y(\mathrm{r},\theta)\big) \rightarrow I(\mathrm{r},\theta)$$

Where I(x,y) is the iris region image, (x,y) are the original Cartesian coordinates, (r, θ) are the corresponding normalised polar coordinates. The rubber sheet model takes into account pupil

dilation and size inconsistencies in order to produce a normalised representation with constant dimensions. In this way the iris region is modelled as a flexible rubber sheet anchored at the iris boundary with the pupil centre as the reference point.

Even though the homogenous rubber sheet model accounts for pupil dilation, imaging distance and non-concentric pupil displacement, it does not compensate for rotational inconsistencies. In the Daugman system, rotation is accounted for during matching by shifting the iris templates in the θ direction until two iris templates are aligned [14].

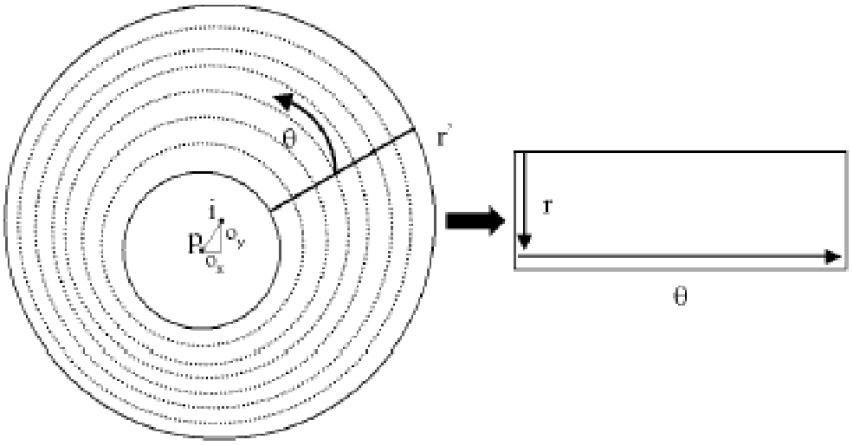

Figure 4.4: Normalization of non-concentric circles.

The points between the inner and outer iris boundaries are interpolated linearly by a homogenous rubber sheet model, which automatically reverses the iris pattern deformations caused by pupillary dilation or constriction. Under assumptions of uniform iris elasticity, this normalization maps the iris tissue into a double-dimensionless coordinate system.

An important aspect of this method of normalization is that it does not introduce unnecessary cuts in the intrinsically continuous and cyclic angular variable, which would interrupt subsequent convolution, as occurs in other methods that explicitly unwrap the iris into a rectangular domain [15].

4.2.3 Iris Template Creation

The iris has a particularly interesting structure and provides abundant texture information. So, it is desirable to explore representation methods which can describe information for an iris. One of the most representative methods is using a two-dimensional Gabor Filter proposed by John Daugman. It is followed by a lot of literature which aimed at further study and improvement of this method [16].

4.2.3.1 2D Gabor Filter

Gabor showed that there exists a 'quantum principle' for information: 'the conjoint time-frequency domain for 1D signals must necessarily be quantized so that no signal or filter can occupy less than a certain minimal area in it'. This minimal resolution, which reflects the inevitable trade-off between time and frequency resolution, has a lower bound in their product. He discovered that Gaussian-modulated complex exponentials provide the best trade-off. Examples of a set of these coherent states or elementary functions are presented in Figure 4.5. This decomposition is equivalent to the Gaussian-windowed Fourier transform. [17]

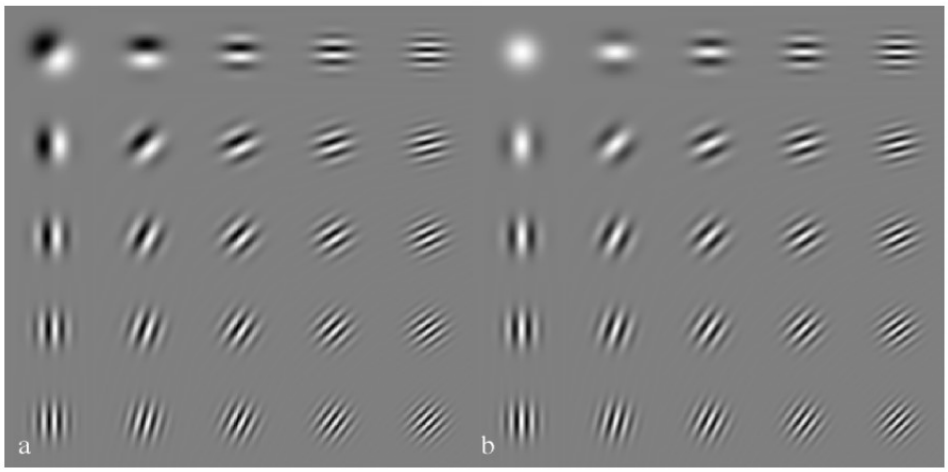

Figure 4.5: An ensemble of odd (a) and even (b) Gabor Filters.

J. Daugman generalized the Gabor function to the following 2D form to model the receptive fields of the orientation-selective simple cells:

$$G(x,y) = \frac{1}{2\pi\sigma\beta} e^{-\pi\left[\frac{(x-x_o)^2}{\sigma^2}+\frac{(y-y_o)^2}{\beta^2}\right]} e^{i\left[\xi_o x + v_0 y\right]}$$

Figure 4.6: 2D Gabor function.

where (x_o, y_o) is the centre of the receptive field in the spatial domain and (ξ_0, v_o) is the optimal spatial frequency of the filter in the frequency domain. σ and β are the standard deviations of the elliptical Gaussian along x and y. The 2D Gabor function is thus a product of an elliptical Gaussian and a complex plane wave. Mathematically, the 2D Gabor function achieves the resolution limit in the conjoint space only in its complex form.

So, a multichannel Gabor wavelet is a set of filter banks with different orientations and different scales. Therefore, a list of parameters must be selected [16]. The frequency

parameters must be selected depending on the pixel resolution, we know the smaller is the frequency less density is extracted.

The angle parameters determine the orientation of the feature extraction. As they are in equal probability distribution in each orientation and the filter is in the specific symmetry in the angular orientation, we can just aliquot angle within the range [0, π].

The scale of filter defining the Gabor in the spatial domain, scale and frequency are inverse proportionally. As explained in above the frequency depends on the size of the image, it works similarly to the scale of filter parameter.

4.2.3 Iris Template Comparison

The template that is generated in the feature encoding process, the iris template creation, gives a feature measure image. Together with the iris template, is needed an iris mask. The iris mask separates the pixels of the iris pattern and the pixels of the eyelids. In this way the algorithm compares only the pixels of the iris pattern [How iris recognition works].

4.2.3.1 Hamming Distance

The comparison between feature measure images gives a matching value, the Hamming Distance. The value is done after implementing a test of statistical independence using a Boolean Exclusive-Or operator (XOR) applied to the bit code image that encode any two iris patterns, masked with AND by both of their corresponding mask bit image to prevent noniris artefacts from influencing iris comparisons. The XOR operator detects disagreement between any corresponding pair of bits, while the AND operator ensures that the compared bits are both deemed to have been uncorrupted by eyelashes, eyelids, specular reflections or other noise. The norms (|| ||) of the resultant bit image and of the AND mask image are then measured in order to compute a fractional Hamming Distance (HD) as the measure of the dissimilarity between any two irises, whose two code iris images are denoted {codeA, codeB} and whose mask bit image are denoted {maskA, maskB}

$$\mathrm{HD} = \frac{\|(codeA \bigotimes codeB) \bigcap maskA \bigcap maskB\|}{\|maskA \bigcap maskB\|}$$

Figure 4.7: Hamming Distance equation

So, the resulting HD is a fractional measure of dissimilarity; 0 would represent a perfect match. The closer to zero is HD more similar are the iris codes. Because any given bit in the code for

an iris is equally likely to be 1 or 0 and different irises are uncorrelated, the expected proportion of agreeing bits between the codes for two different irises is HD = 0.500. The histogram in Figure 4.8 shows the distribution of HDs obtained from 9.1 million comparisons between different of iris images. Their observed mean HD was p = 0.499 with standard deviation σ = 0.0317.

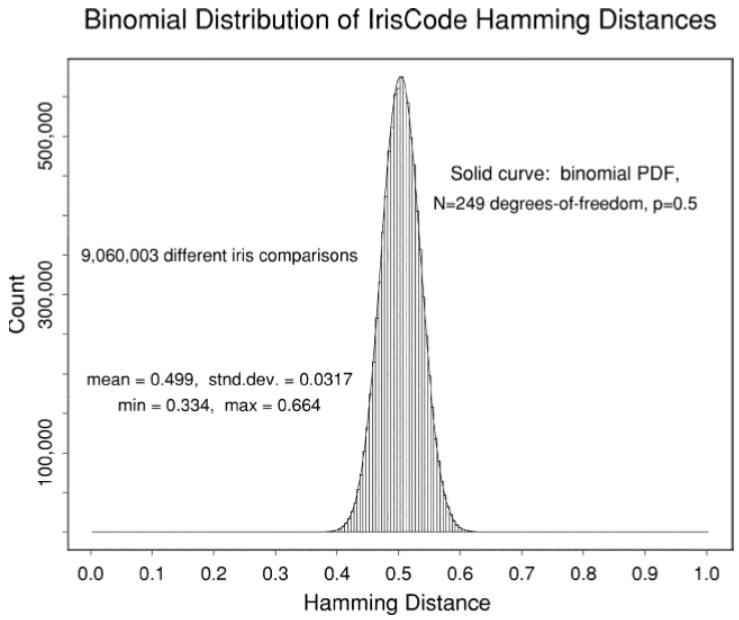

Figure 4.8: Distribution of HDs from all 9.1 million possible comparisons between different pairs of irises in the database.

4.2.3.2 Decision Environment for Iris recognition

The overall 'decidability' of the task of recognizing persons by their iris patterns is revealed by comparing the HD distributions for same versus for different irises. In figure 4.9 is shown the different HD distributions. The mean of the 'same' distribution was p = 0.110 and the standard deviation was σ = 0.065. In order to obtain a final result of the comparison as match or non-match, a threshold is needed. In case of using a database is possible to obtain the suitable threshold to minimize the match error.

Obviously, establishing a threshold is an essential step in the system and it determines the accuracy of the system. The developer can choose the threshold depending on the environment of the system. For example, if we don't want to have match errors we should increase the threshold. Increasing the threshold means to increase the non-match errors and decrease the match errors.

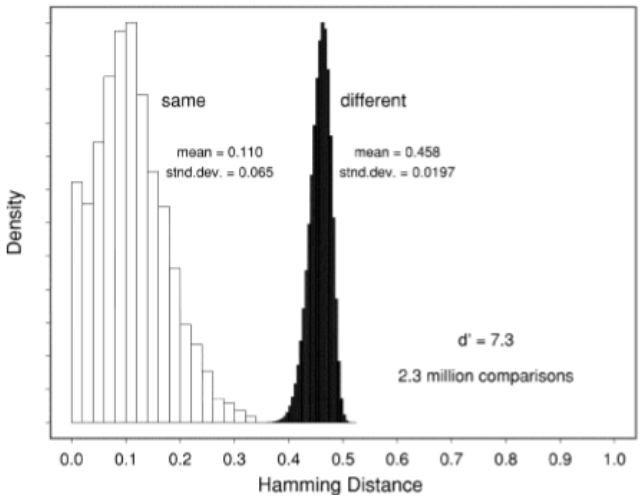

Figure 4.9: HD distributions of a database with irises of same and different persons

CHAPTER 5

Proposed Iris Recognition Method

This chapter describes the following proposed iris recognition methods:

- Iris Segmentation
  - Fit ellipse method – Pupil Boundary
  - Finding the iris radius – Iris Boundary
- Iris Normalization
  - Warping method
  - Eliminating eyelids
  - Image Enhancement

The proposed iris segmentation methods perform image processing to find the iris pattern. Given a grayscale sample image they produce both an accurate pupil and iris boundary. These methods work for all types of images described in the chapter 3, off-axis orientation, different size and eyelid occlusion.

The proposed iris normalization methods perform image processing to normalize the segmented iris and make the necessary changes to the iris pattern in order to obtain the best quality to perform the iris comparison.

In figure 5.1 is shown the system overview. It shows the system structure, and shows how it works in general.

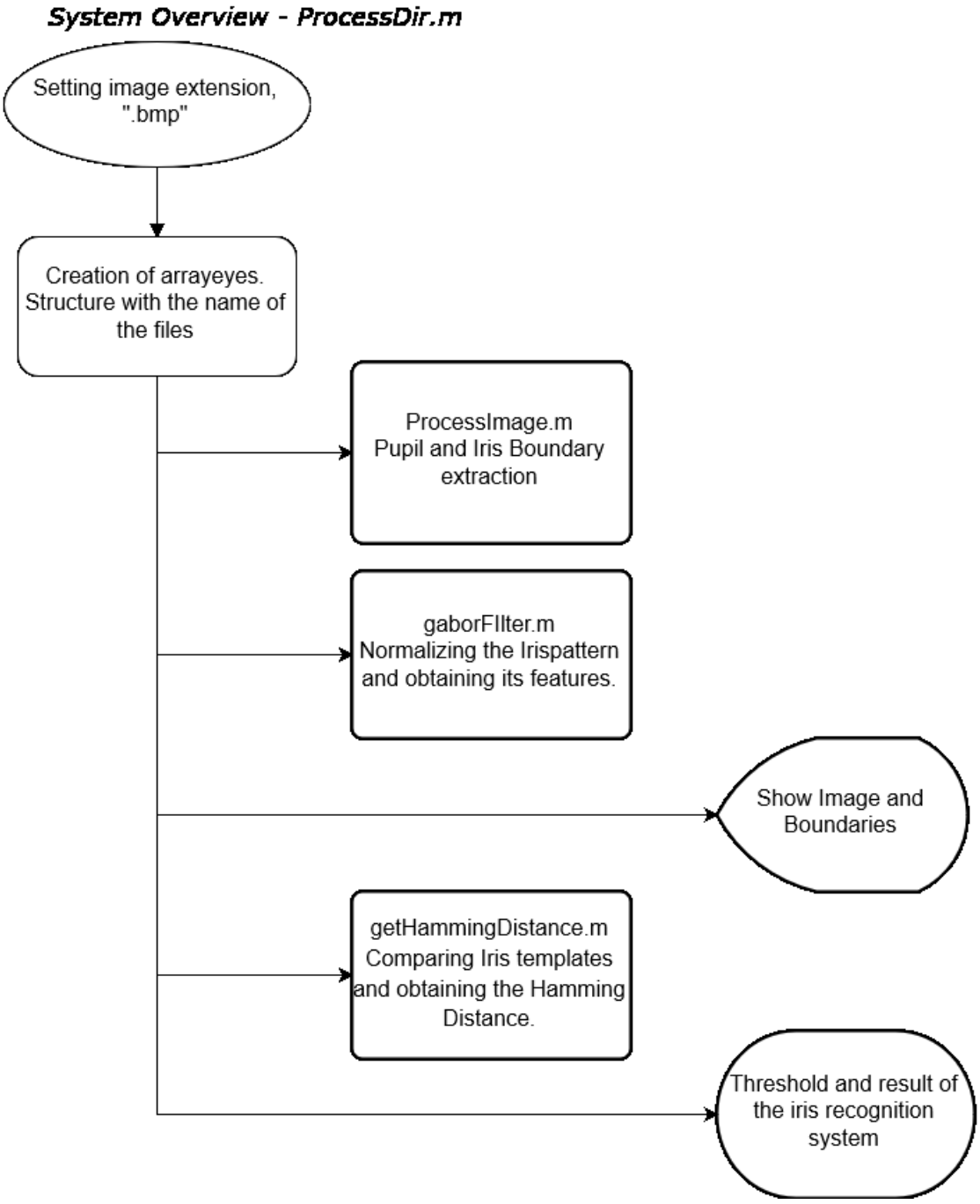

Figure 5.1: System Overview flowchart

5.1 Iris Segmentation

Before starting designing the iris segmentation methods is interesting to take a look into all the database images we are going to work with. In the CASIA database there are some issues that we have to discuss. Such are the contrast, the subject distance to the lens of the camera, the eye structure, etc.

The first discussion is about which boundary we have to process first, the pupil or the iris boundary. The meaning of 'pupil boundary' is the separation between the pupil and the iris pattern, and the meaning of 'iris boundary' is the separation between the iris pattern and the sclera. If we look at the images, we notice that the contrast is bigger at the pupil boundary. The pupil is likely the darkest area in the image, is easier to detect the pupil boundary than the iris boundary. This is the reason why algorithm starts finding the pupil boundary.

In figures 5.2 and 5.3 are shown the iris segmentation system flowcharts. In figure 5.2 is shown the pupil boundary extraction with its inputs and outputs. The inputs of the pupil boundary method are the eye image and predefined parameters. In figure 5.3 is shown the iris boundary extraction. The inputs o the iris boundary method is the eye image, the pupil boundary and predefined parameters.

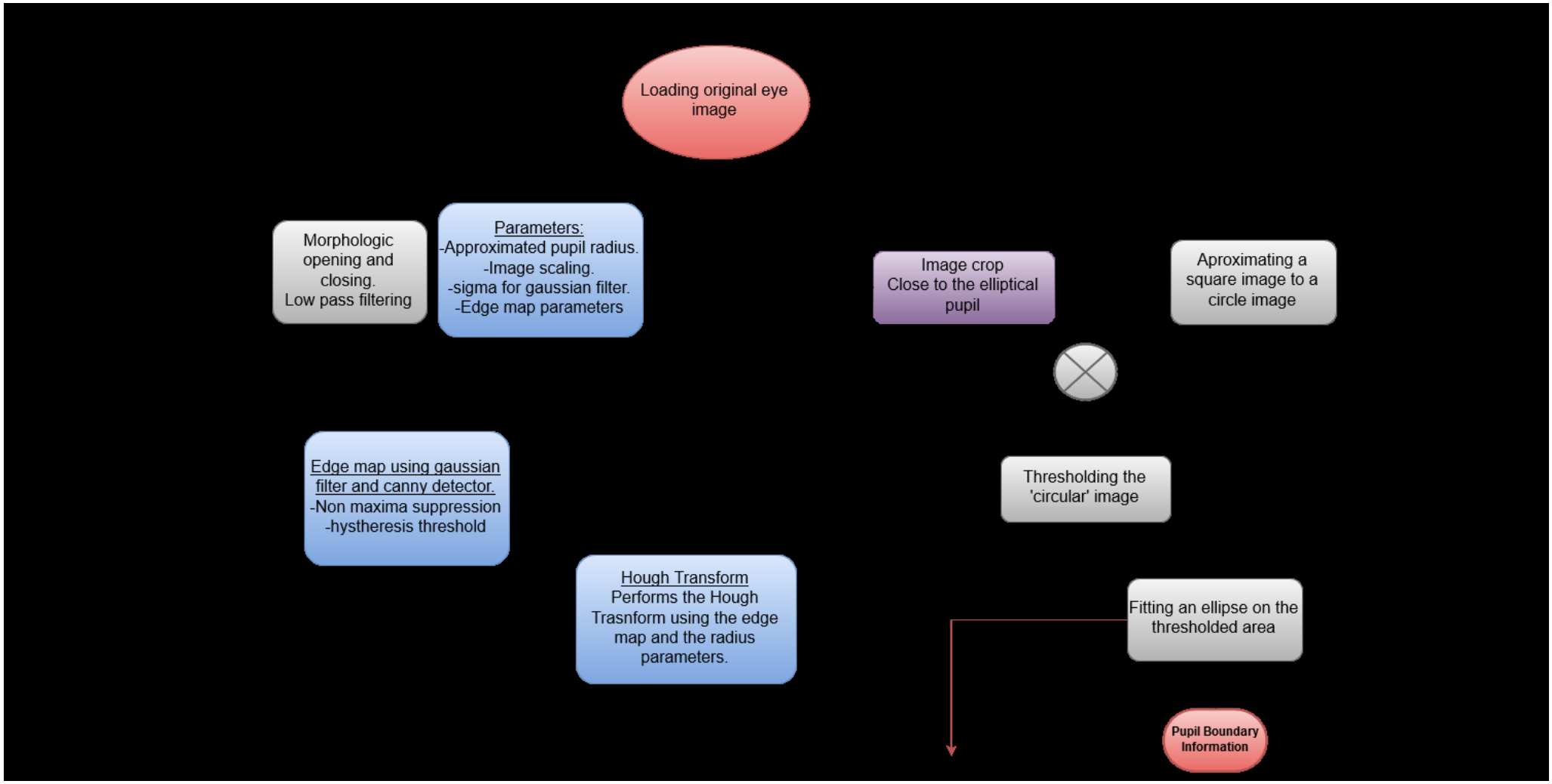

Figure 5.2: Pupil boundary extraction flowchart

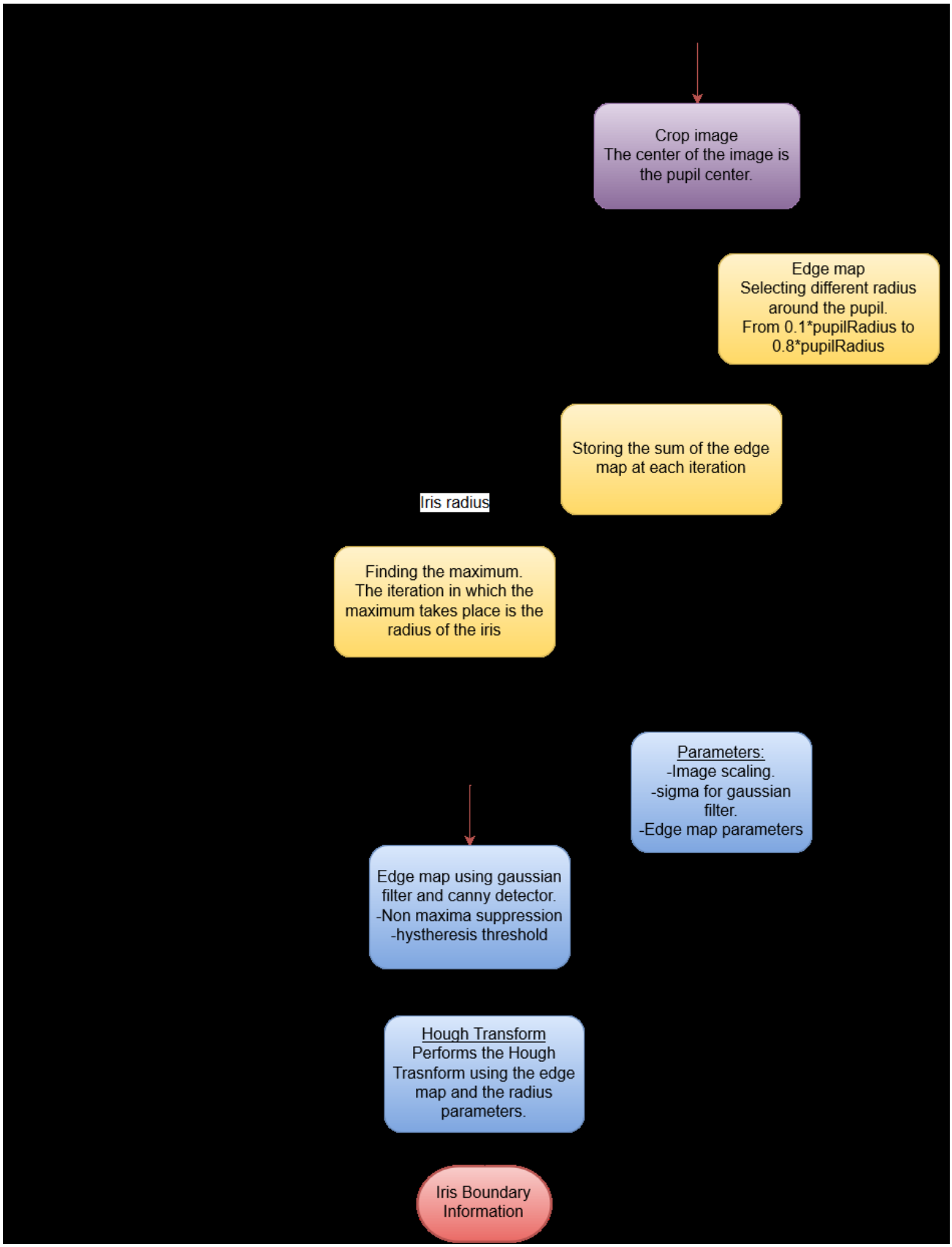

Figure 5.3: Iris boundary extraction flowchart

5.1.1 Pupil Boundary

At this stage of the algorithm there is no information about the image, we just have the image to process. To obtain a good segmentation, there are some factors to keep in mind.

1. The dark pigmentation of the iris decreases contrast between the iris and the pupil.
2. The iris is a rough surface.
3. The pupil is approximately a circle.
4. In some images the eyelids occlude the pupil surface.

These factors are really important during the process of designing the method. Firstly, an image pre-processing is needed. The reason is that the iris is a rough surface and we want smooth surfaces, also we want to eliminate the eyelids.

To obtain smooth surfaces some morphologic opening and closing are performed. The morphologic opening is the dilation of the erosion of an image by a predefined structuring element. Opening removes small objects from the foreground (usually taken as dark pixels) of an image. The morphologic closing is the erosion of the dilation of an image by a predefined image. Closing removes small bright elements. Altogether, the morphologic opening and dilation eliminate the small objects and leaves unchanged the big objects.

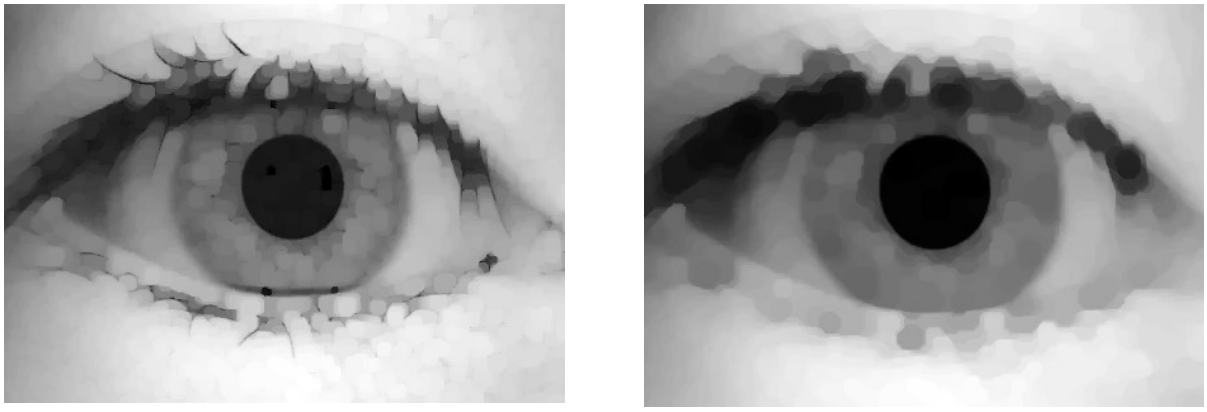

Figure 5.4: From left to right, opening to the original image and closing to the 'opened' image

The structuring elements are disks with radius 6 and 8, for opening and closing respectively. Obviously, the radius is predefined and it's the same radius for all the samples. The most suitable structuring element radius is not the same for all the images, but we have to choose the most suitable structuring element radius for the most of the samples.

5.1.1.1 Hough Transform

The Hough Transform is a standard computer vision algorithm that can be used to determine the parameters of simple geometric objects, such as lines and circles, present in an image. The circular Hough transform can be employed to deduce the radius and the centre coordinates of the pupil region. From the edge map, votes are cast in Hough space for the parameters pf circles passing through each edge point. These parameters are the centre coordinates x_c and y_c, and the radius r, which are able to define any circle according to the equation [18].

$$x_c^2 + y_c^2 - r^2 = 0$$

A maximum point in the Hough space will correspond to the radius and centre coordinates of the circle best defined by the edge points. To implement the Hough transform algorithm some changes were done. Knowing that the Hough space it's made up of parameters, setting up parameters should minimize the errors and the time consumption of the method. We are going to set up the radius parameter because we know approximately the radius of the pupil. In chapter 7 some statistics about the pupil size are shown. In this way, the possible radiuses are 28 to 55 pixels. In figure 5.5 it's shown an example of the Hough space in which the whiter pixel corresponds to the best defined circle. This image represents the Hough space parameters, the x axis corresponds to the x position of the pupil centre and the y axis to the y position of the pupil centre. The drawn circles correspond to one specific radius from 28 to 55 pixels. In fact, there are 27 images like this one for each specific radius. The obtained parametric result is the whiter pixel in the 27 images.

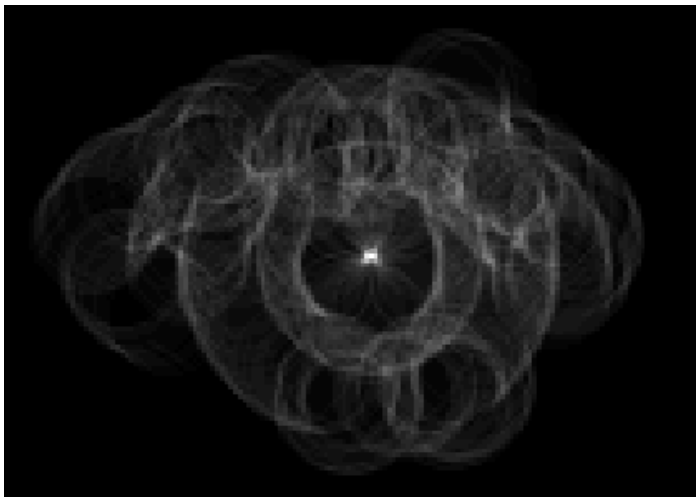

Figure 5.5: Hough space of a certain radius

There are a number of problems with the Hough transform method. First of all, it requires threshold values to be chosen for edge detection, and this may result in critical edge points being removed, resulting in failure to detect circles. Secondly, the Hough transform is computationally intensive due to its 'brute-force' approach. In order to do an efficient algorithm, a process of image scaling is developed. In this case, it has been decided to convert the image from 480*640 pixels to 144*192.

After this explanation about the Hough transform, it is understood the importance of the edge map. If the edge map has more edge points than needed, the procedure will be slow because of Hough transform. To perform the edge detection step. Derivatives in horizontal and vertical directions are performed.

The canny edge detector is used to obtain the edge map. This method is a multi-stage algorithm to detect a wide range of edges in images. The algorithm works by finding the intensity gradient in the image. An edge in an image may point in a variety of directions, so the canny algorithm uses two filters to detect horizontal and vertical edges in the image.

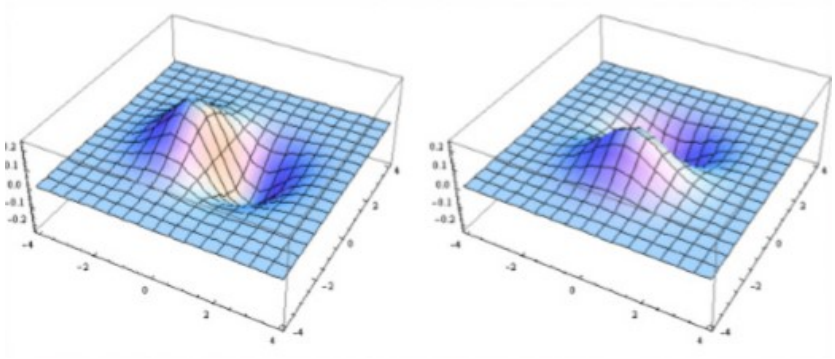

Figure 5.6: Canny edge detector filters to detect horizontal and vertical edges.

In figure 5.7 its shown different edge maps using one or another filter. In this case, the different edge maps have different uses. At this stage of the algorithm we want to find the pupil. If the pupil is occluded by the eyelids the horizontal information of the pupil is occluded, so that the vertical information of the pupil is more important.

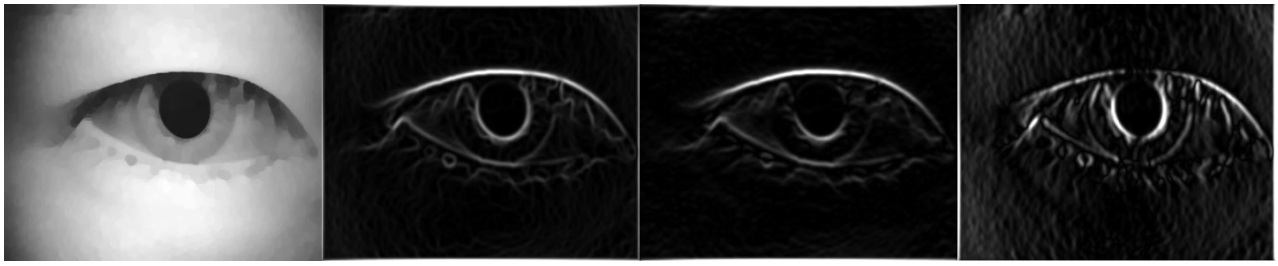

Figure 5.7: From left to right, Enhanced image, Edge map, Horizontal edge map and Vertical edge map

Combining the information of edge maps, we can obtain the best edge map for performing non-maxima suppression followed by hysteresis thresholding [19]. Non maxima-suppression is an edge thinning method. After applying gradient calculation, the edge extracted from the gradient value is still quite blurred. With respect of the criteria, there should only be one

accurate response to the edge. Thus non-maxima suppression can help to suppress all the gradient values to 0 except local maxima, which indicates location with the sharpest change of intensity value.

So far, the edge map has been thinned, a hysteresis thresholding should be developed because the canny method also extracts weak edge pixels. But, the weak edge pixels can also be part of the real edge. To achieve an accurate result, the weak edges near to strong edges should be kept but the others not. Usually, a weak edge pixel caused from true edges will be connected to a strong edge pixel while noise responses are unconnected. To track the edge connection, blob analysis is applied by looking at a weak edge pixel and its 8-connected neighbourhood pixels. As long as there is one strong edge pixel is involved in the blob, that weak edge point can be identified as one that should be preserved.

In order to develop the hysteresis thresholding, two threshold values are needed. Determining the threshold values is really important. If the threshold values are too big the pupil boundary would be determined as a weak edge and turned to zero. In figure 5.8 is shown the procedure to obtain the real edge.

Figure 5.8: From left to right, Edge map obtained using canny method, non-maxima suppression image, hysteresis thresholded image.

The Hough transform uses the hysteresis thresholded image to find a circle. That is why it's not necessary to threshold all the pupil circle, just having a part of the circle is enough. Because the algorithm searches the best fitted circle of certain radius. In this case, is interesting due to eyelids occlusion. It's not possible to threshold all the entire circle.

In figure 5.9 it's shown some examples of the result the Hough transform gives. We can see that the result the Hough transform gives is not accurate. To perform a good iris recognition system an accurate pupil boundary should be performed, because the centre of the pupil should be the centre of the Daugman's rubber sheet model.

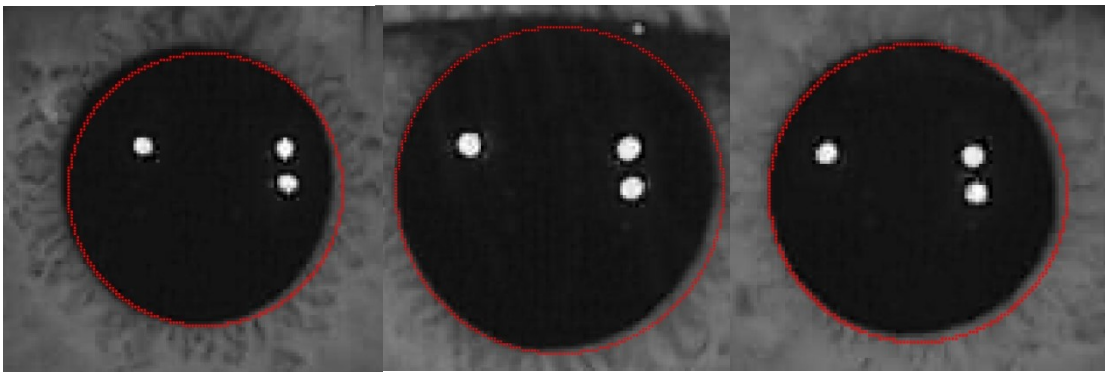

Figure 5.9: Enlarged image of the pupil with the calculated pupil boundary

5.1.1.2 Fit Ellipse method

The state of the art assumes that the pupil is a circle, with its centre and radius. But really, ophthalmology says that the pupil is not a 'perfect circle', it has irregularities around its boundary. Despite what is the real pupil, in terms of image processing if the pupil is looking into the lens of the camera the pupil is a circle.

But, the camera is obtaining one projection of the eye, Figure 5.10. The projection of the pupil would be a circle if the subject looks into the lens of the camera. Making an empirical study of the images we realise that the projection of the eye is an ellipse, because the subject doesn't look into the lens of the camera. Thereby, we are going to use the circle calculated by Hough Transform and the information of the image to define an accurate ellipse.

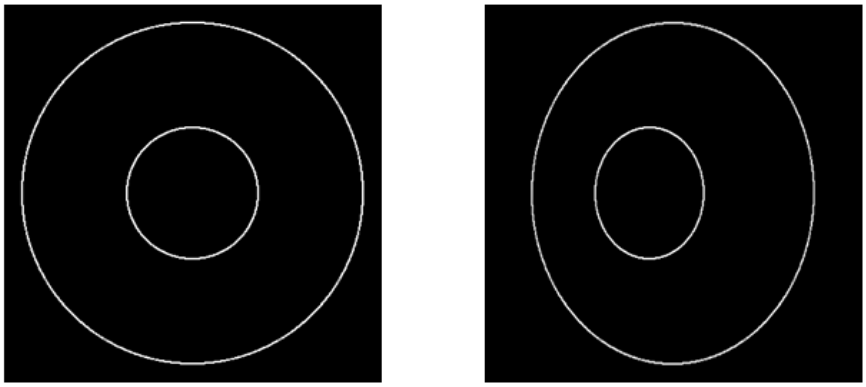

1. Model of the eye looking into the lens of the camera.

2. Model of the eye looking at the left of the lens of the camera.

Figure 5.10: Differences between eye model and its projection

The method starts by cropping the image in order to select the pupil information. Once we have the image cropped, is time to enhance the image. At this stage the image consists of black area for the pupil and grey are for the iris pattern as seen in figure 5.11. As did in the Hough transform method we are going to enhance the image by applying opening and closing.

The pupil is circular but the image is rectangular, so that part of the image is unnecessary for the process. In this way, the pixels farther to the centre of the image (the centre of the image is the centre of the pupil calculated by the Hough Transform)

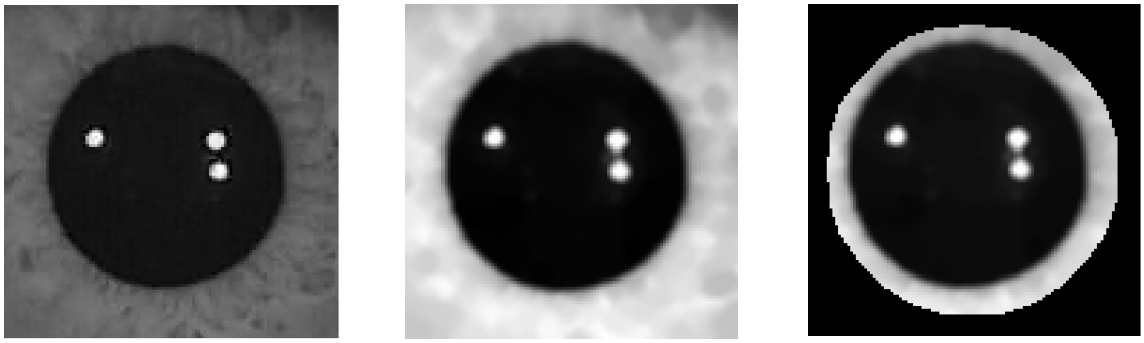

Figure 5.11: From left to right, cropped image, enhanced image
and circular cropped image

It's known that the pupil is darker than the iris pattern, that's why a threshold is used. Using Otsu's method to find the best way to separate the histogram makes automatic the process of thresholding, and it doesn't depends on the illumination. The specular reflections are thresholded as iris pattern because there are lighter than the pupil. Therefore, a fill holes method is developed. Finally, the algorithm 'Fit ellipse' approximates an ellipse into the surface by minimizing geometric distance, a nonlinear least square problem [20].

Least squares is a standard approach in regression analysis to the approximate solution of over-determined systems. Consider a set of data, the sum of error measure (distance from the points to the ellipse) is minimized by changing the parameters of the ellipse. Using a convergence criteria the parameters are chosen. The common sense criterion for convergence is that the sum of squares does not decrease from one iteration to the next. However, this criterion is often difficult to implement in practice. So that an approximation is needed.

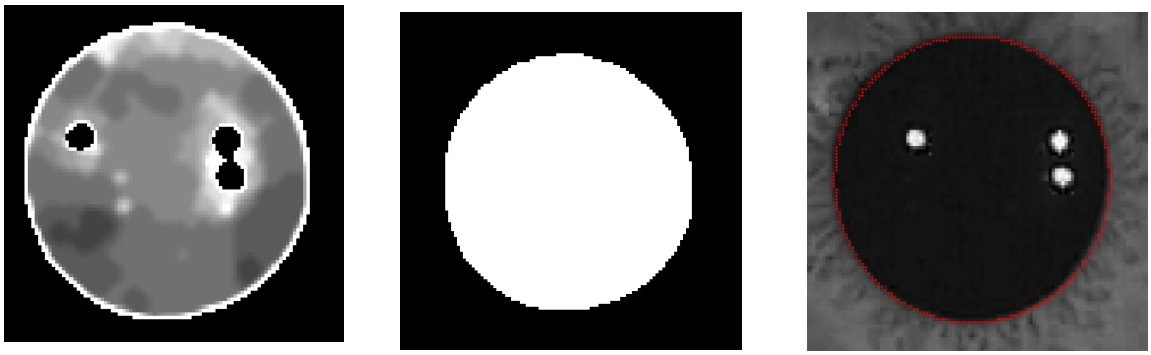

Figure 5.12: From left to right, thresholded image, hole filled image and final fitted ellipse on original image.

5.1.2 Iris Boundary

In the proposed method to find the iris boundary some things must be taken into account to optimize the algorithm. Is possible to optimize the algorithm because:

1. In the database of iris images, such as CASIA, the minimum and maximum size of the irises can be estimated by observing a training set.
2. The centres of pupil and iris in such database are near to the centre of the image.
3. There is a relation between the size of iris and pupil.
4. The centres of pupil and iris are in the same position or close enough.

At this stage, we know how the radius and centre of the pupil are. And, we can use this information to find the iris boundary. The iris radius is 1.25 to 10 times bigger than the pupil radius [1]. And the pupil centre and iris centre are approximately at the same position.

In the pupil boundary section, it is said that the image is a projection of the reality. This change also influences the distance between the pupil centre and the iris centre. If the eye is looking into the lens of the camera the centres are approximately in the same place.

We are going to work with the circular Hough Transform again to find the iris boundary. But, in this case the contrast between the sclera and the iris pattern is lower. So, we have to use a modified edge map to the Hough Transform eliminating all the edges that are not the iris boundary. In this way, we are going to reduce the possible radius that the Hough Transform iterates.

5.1.2.1 Finding Iris Radius

We are going to find the iris radius assuming that the position of the centres of the iris and the pupil are the same. The Hough Transform is the responsible for finding the exact position of the centre. So, the aim of this stage is finding the iris radius.

Firstly, it's known that the iris boundary radius is 1.5 to 10 times bigger than pupil radius. So, the algorithm starts by finding an approximate iris radius on this range. Before that, in Figure 5.13 is shown the region of interest to find the iris radius. It can be seen that the surface between the pupil boundary and the iris boundary is steady. Because the iris pattern is an unchanged grey surface with any abrupt areas.

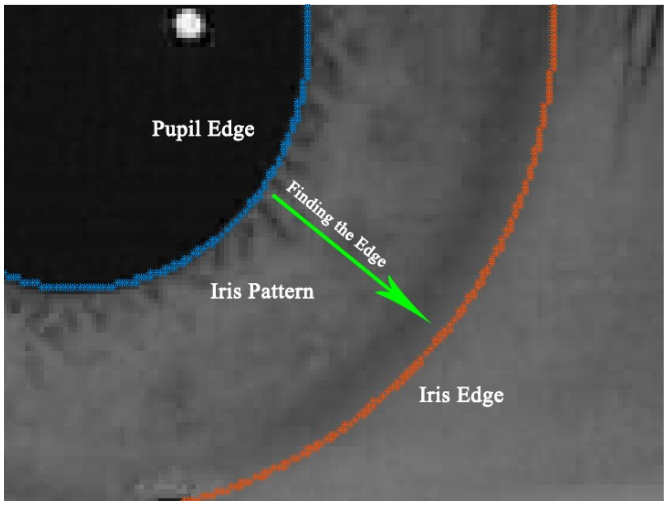

Figure 5.13: Term definition and surface differences

We can see that if we increase the radius of the pupil boundary, the next edge that we found is the iris edge. So that, in order to find the iris edge the algorithm compares the edge of different radius and chooses the one with more edge information. To compare the edge information we sum the edge pixels in each iteration. The maximum of the series is the iris edge. In figure 5.14, we can see the used image to do the iris radius finding process. The top of the image is missed because the eyelids are inconvenient to the process.

Figure 5.14: Cropped Edge map used in the process and
one iteration of the process

5.1.2.2 Circular Hough Transform

The Hough Transform provides a circle with its centre and radius, and we said in the previous stage of the algorithm that the pupil is an ellipse because of the characteristics of the image. In this case, it's different. The dimensions of the iris are bigger. So, the transformation of the iris due to its projection affects less to its features. Hereby, we assume that the iris is circular.

To obtain a good result of the Hough Transform is important to give an edge map of the region of interest. The algorithm adjusts a circle around the iris edge map with the information of the iris radius. In figure 5.15 it's shown the procedure and the adjustment. Obviously, the adjusted circle around the iris that was obtained by the iris radius method is an approximate circle. The iris boundary has to be within the 'doughnut'.

Figure 5.15: Selection of the Edge Map using the information of the iris radius
and the position of the pupil centre

The Hough Transform works in the same way as before. It uses canny method, non-maxima suppression and hysteresis thresholding. At this time, what changes in the Hough Transform algorithm is the Hough space. A limitation is developed in order to obtain a good result. It's known that the centres of the boundaries are close, so that the Hough space has a condition and only circles with certain centre position are taken into account. In figure 5.16, it's shown the condition of the Hough space using segmentation.

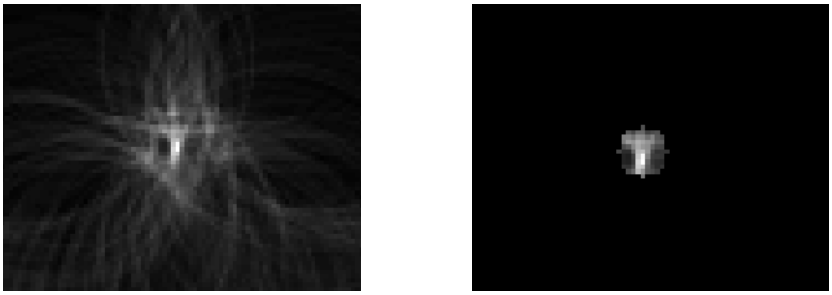

Figure 5.16: From left to right, complete Hough space and segmented Hough Space.

Finally, the Iris pattern is segmented. In chapter 7 some results are discussed and some images shown. As seen in figure 5.17, the iris pattern can be segmented using both boundaries. In iris normalization a method for eyelids and skin is developed.

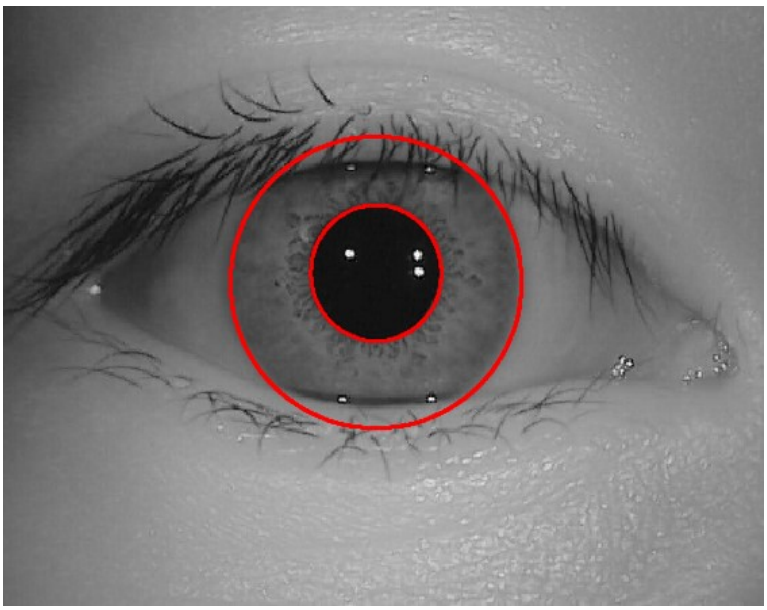

Figure 5.17: The iris and pupil boundary on the iris image.

5.2 Iris Normalization

Once the iris region is successfully segmented from an eye image, the next stage is to transform the iris region so that it has fixed dimensions in order to allow comparisons. The dimensional inconsistencies between eye images are mainly due to the stretching of the iris caused by pupil dilation from varying levels of illumination. Other sources of inconsistency include, the distance between the camera and the subject, rotation of the camera, head tilt, rotation of the eye within the eye socket, and the change of pupil position regarding the iris. The normalization process will produce iris regions, which have the same constant dimensions, so that two images of the same iris under different conditions will have characteristic features in the same spatial location.

In figure 5.18 is shown iris pattern normalization flowchart. It uses the iris and pupil boundary to segment and normalize the iris. The iris extracting features are included in flowchart.

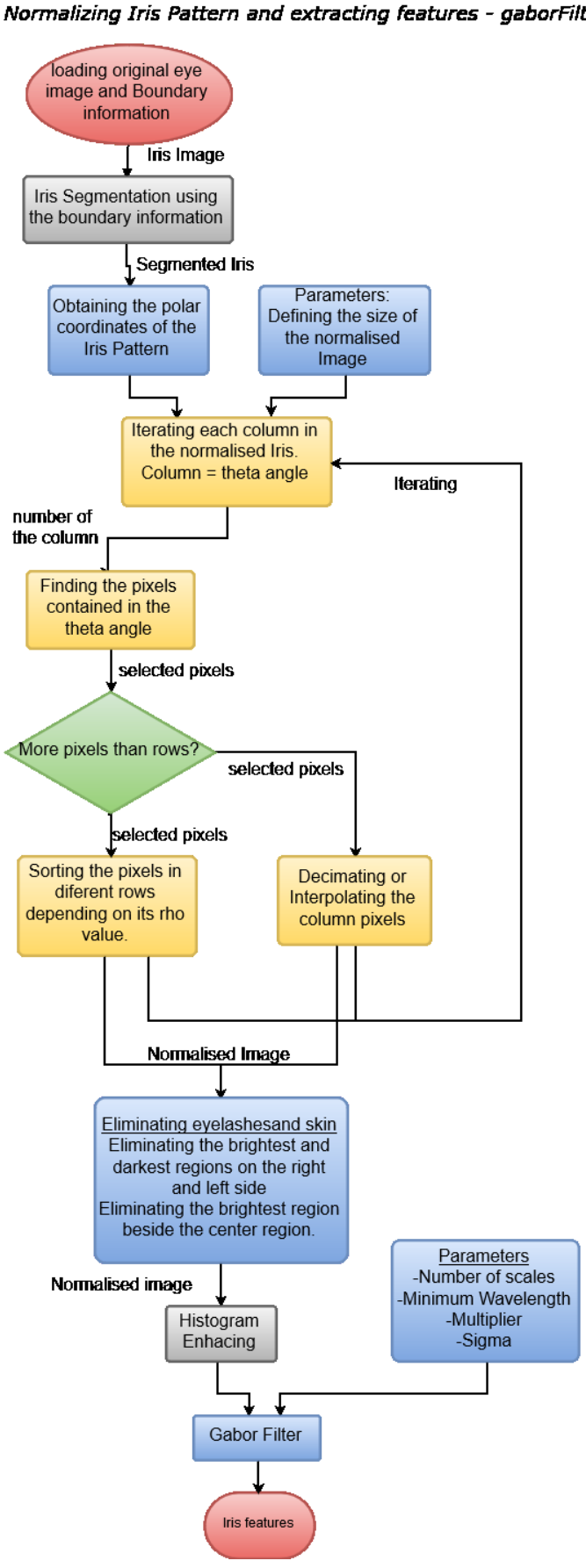

Figure 5.18: Iris normalization and feature extraction flowchart

5.2.1 Daugman's rubber sheet model

The algorithm follows the state of the art Daugman's rubber sheet model to normalize the segmented iris. It has been widely tested in several situations, and it's a good solution to solve the inconsistencies between samples. The homogeneous rubber sheet model accounts for pupil dilation, imaging distance and nonconcentric pupil displacement. It does not compensate for rotational inconsistencies. Besides, a solution is developed.

In the procedure to remap the iris region to polar coordinates a warping method is used to have a constant diameter so that when comparing two samples, both are considered as Daugman's rubber sheet model, see chapter 4. This works for every when attempting to match to iris regions. Every iris region is normalized and saved with the same dimensions by storing the intensity values along virtual concentric circles. A normalization resolution is selected, so that the number of data points extracted is the same.

This method resolves the warping problem by normalizing the 'doughnut' radius of each θ direction. In figure 5.19, it's shown the different θ directions with different radius.

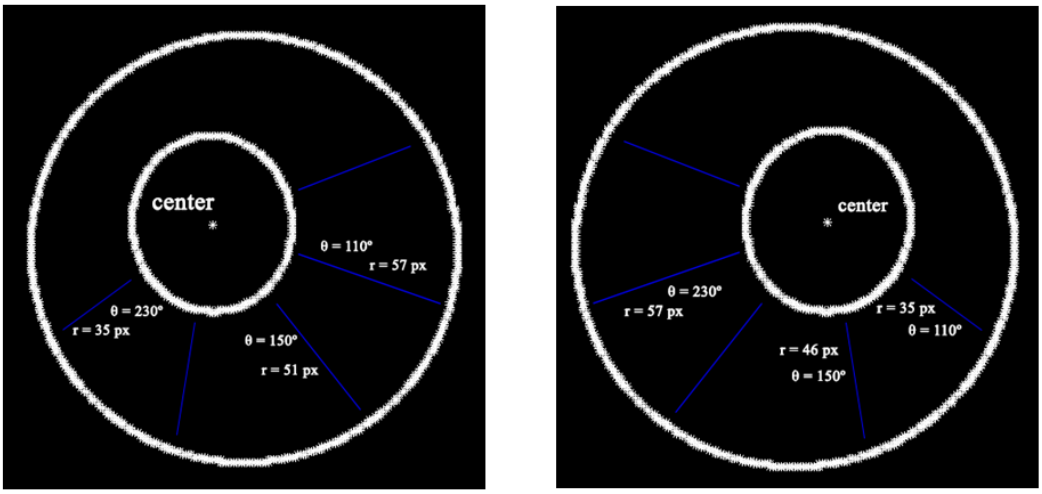

Figure 5.19: Iris 'doughnuts' with different pupil positions.

So, an angular resolution and a radial resolution are needed. Basically, it means that the method has a fixed image resolution. In this method, the resolution of the normalized image is 65*260 pixels, is an angular resolution of 260 pixels and a radial resolution of 65 pixels. Having 260 pixels of angular resolution is equal to separate the 360º of the image in 260 equal parts, and to separate the variable radius in 65 equal parts.

5.2.1.1 Warping Method

The aim of the warping transformation is to obtain the same image regardless the position the subject is looking to. As we can see in the figure 5.19 the radial resolution changes depending on the angular position and the position of the pupil. Obtaining the concentric circles is equal to obtain an image as the physiologically eye. Without warping, images of different positions of the pupil would fail.

The method works by transforming column by column (angular position from 1 to 260). The method is modelled as:

$$WarpedRho = \frac{Rho}{RhoGap} \quad 5.1$$

$$RhoGap = \frac{\max(Rho) - \min(Rho)}{RhoResolution} \quad 5.2$$

Where *WarpedRho* is the position of the warped column from 1 to 260, *Rho* is the original position of the column, and *RhoResolution* is the length of the warped column (equal to 260).

This is how the values are obtained for each column and row. But, the number of pixels of the original image is uncertain. Normally, there are more pixels in the original images than gaps in the normalized image. So, a transformation is needed. If there are several values for each gap we would decimate the values so that they fix into the new image. Otherwise, a interpolation is developed. In figure 5.20 it's shown explained with an image the process of a unique column. Highlighted in red is shown the transformation, from polar to rectangular shape.

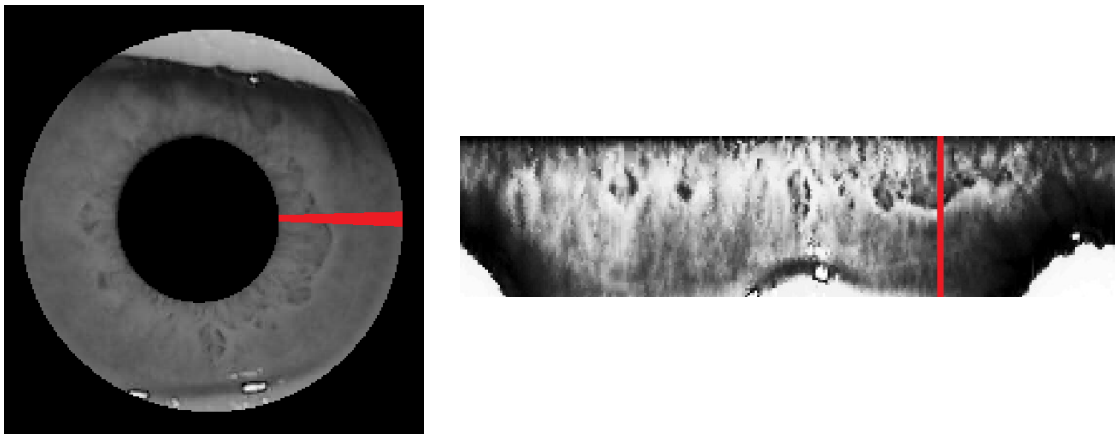

Figure 5.20: From left to right, segmented image and normalized image.

5.2.2 Eliminating eyelids

Once we have the iris pattern normalized is time to ameliorate the image to get the best matching. The iris pattern is treated as noise, so if there are other elements in the image they can't be treated as noise. So, we have to eliminate the information related to skin and eyelashes.

As seen in figure 5.20, the eyelashes and eyelids are located in certain positions. In the centre and sides of the image. Also, these parts are the darker and lighter parts in the image because the iris pattern is a grey surface. We are going to threshold these parts.

The matching algorithm has two inputs, the enhanced iris pattern and the mask. The mask shows which pixels is the iris pattern and which isn't. The state of the art algorithm uses this mask to avoid the information that is not the iris pattern. It is said that if in one image there's beside occlusion and in other above occlusion the comparison would be really complicate. It would be complicate because the iris region left to compare is narrow.

As seen in figure 5.21, the white pixels are the iris pattern and the black pixels are the eyelids. As said above, the comparison algorithm ignores the black pixels so that the region of interest is the central surface.

Figure 5.21: Iris mask

5.2.3 Image Enhancement

Finally, image enhancement is developed in order to obtain a good histogram of the image. Normalizing the histogram is good for illumination variations because it normalize the DC energy.

Firstly, a histogram adjustment process is developed by normalizing the histogram. To adjust the histogram means to put the darkest pixel as 0 and the lighter pixel as 1. We do this because all the pixels on the iris pattern surface are rather gray in a narrow margin.

Secondly, histogram equalization is improved. To equalize the histogram is to distribute the intensities through all the histogram. In figure 5.22 we can see the original iris pattern and in the figure 5.23 the enhanced image.

Figure 5.22: Original Iris pattern

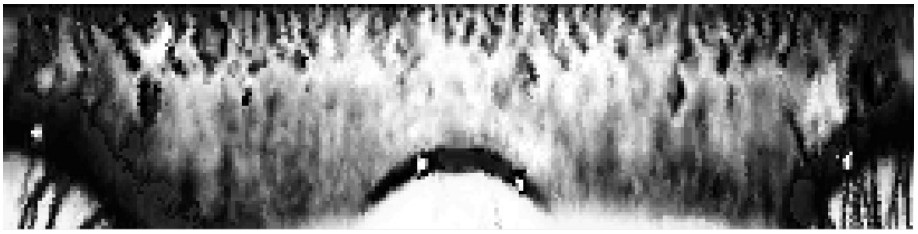

Figure 5.23: Enhanced Iris pattern

CHAPTER 6

Experimental Setup

The iris detection and normalization algorithms are fully implemented in MATLAB. It is a procedural language, combining an effective programming structure with a bevy of predefined mathematical commands [21]

MATLAB is extremely effective, when performing computations on matrices, the main data structure. It comes with “toolboxes”, tools to implement more efficiently image processing, data signal processing and various other algorithms.

6.1 Experimental Setup

The main reason this was the chosen implementation language, is the tools in the image processing toolbox MATLAB provides, set of predefined commands for image editing and preprocessing. The ones used in the development of the algorithms are:

- imread() – reading an image from file.
- imadjust() – contrast improvement.
- imfill() – hole filling algorithm.
- imresize() – image resizing.
- imopen() – morphological opening on a grayscale image.
- strel() – creates a morphological structuring element.
- imshow() – displaying an image on the screen.

All images are represented as matrices, where every cell of the matrix represents a pixel in the image. The manipulation is very easy, because values can be directly accessed by specifying the indices in the matrix. The origin of the coordinate system is the top left corner, where the x-axis stretches horizontally to the right and the y-axis stretches vertically to the bottom.

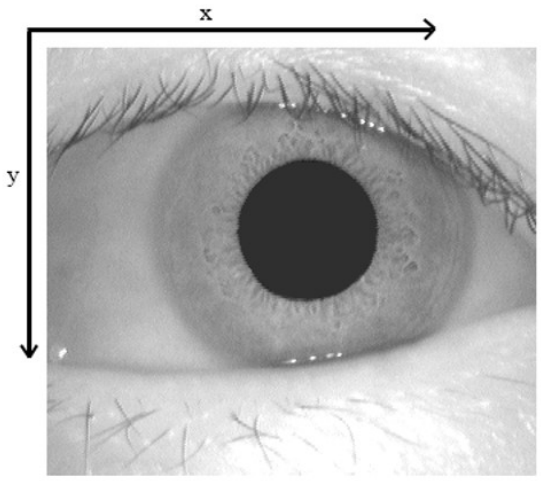

Figure 6.1: Coordinate system

6.2 Structure

The project has a modular structure and the iris segmentation, normalization and matching are put in separate scripts. Because of this structure the algorithm can be separated, knowing the inputs and outputs needed. To show the results MATLAB provides a Handle Graphics.

CHAPTER 7

Experimental Results

This chapter describes the results obtained from executing the experiment procedure described in chapter 5.

Firstly, statistics of iris segmentation method are described and analysed. Then, statistics of iris normalization and enhancement are shown. Finally, statistics of comparison are discussed. Those statistics are from the images of CASIA iris v2 database. A discussion about the database is shown below.

Tests were carried out to find the best separation, so that the false match and false accept rate is minimized, and to confirm that iris recognition can perform accurately as a biometric for recognition, experiments were also conducted in order to confirm the uniqueness of human iris patterns by deducting the number of degrees of freedom present in the iris template representation.

There are a number of parameters in the iris recognition system, and optimum values for these parameters were required in order to provide the best recognition rate. These parameters include; the radial and angular resolution, r and ϑ respectively, which give the number of data points for encoding each template. Also, the filter parameters include, the number of filters, N, their base wavelength λ, and the multiplicative factor between centre wavelengths of successive filters. Also examined were the numbers of shifts required to account for rotational inconsistencies between any two iris representations.

7.1 Statistics of Iris Segmentation

7.1.1 Pupil Detection

The performance of the proposed Fit ellipse method is shown for different types of eye images in Figure 7.1. In the figure 7.2 are shown the possible errors of the algorithm.

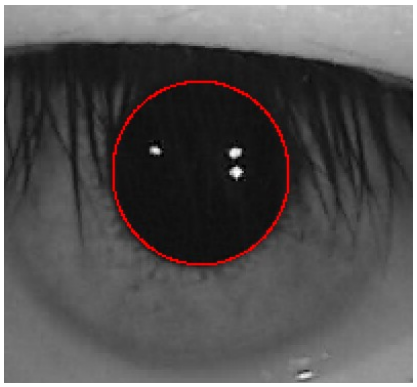

(a)

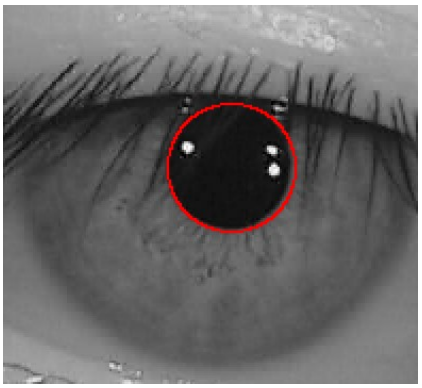

(b)

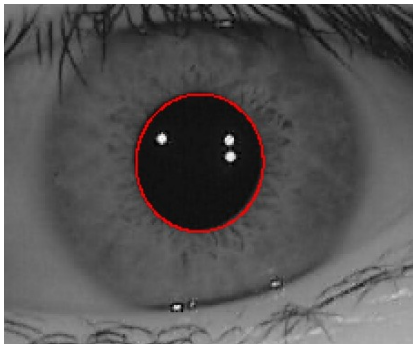

(c)

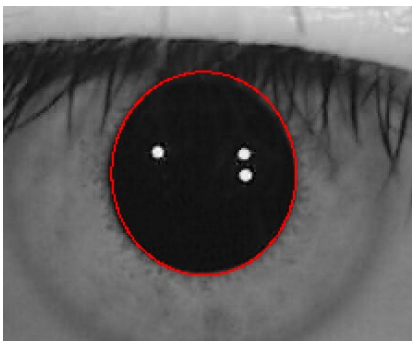

(d)

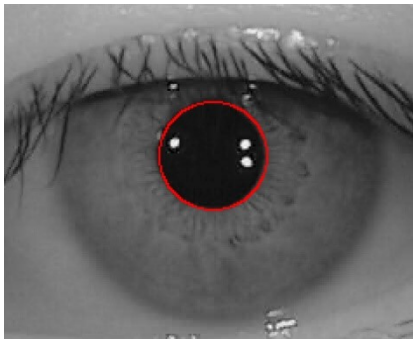

(e)

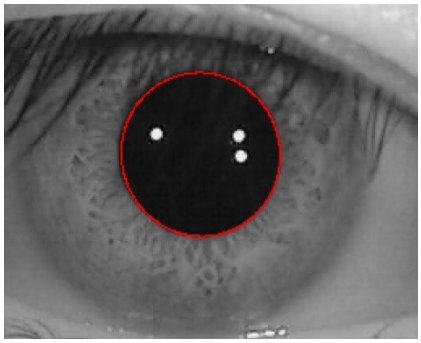

(f)

Figure 7.1: (a)-(f) illustrate the results of pupil detection using the Fit Ellipse method. The red ellipse shows the calculated result. This set of results show the well localized pupil boundary.

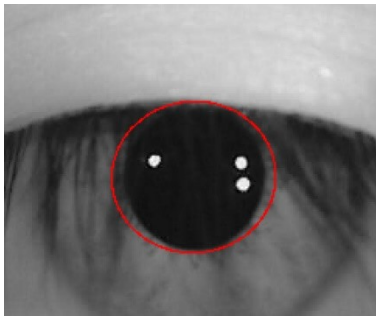

(a)

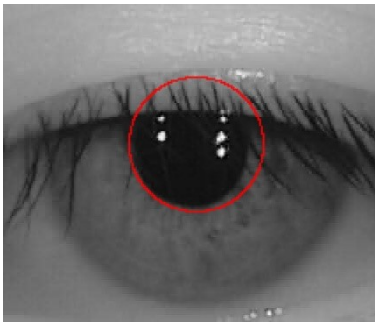

(b)

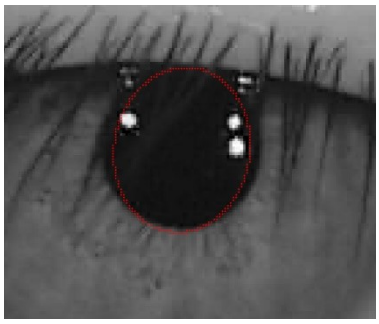

(c)

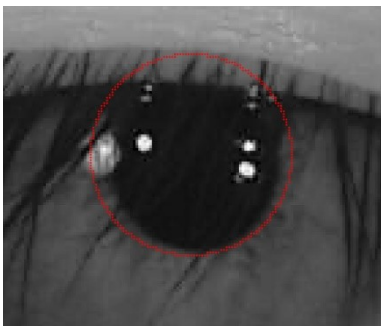

(d)

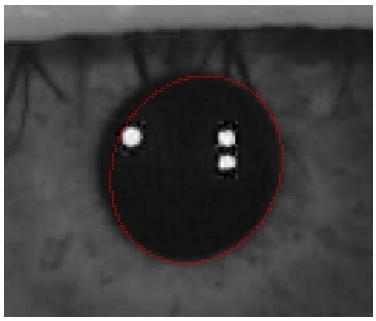

(e)

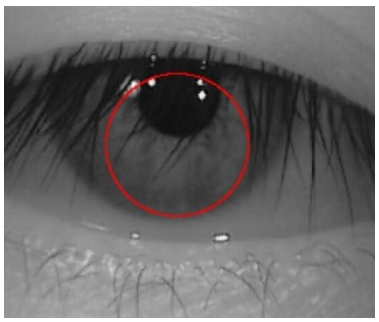

(f)

Figure 7.2: (a)-(f) illustrate the results of pupil detection using the Fit Ellipse method. The red ellipse shows the calculated result. This set of results show the bad localized pupil boundary.

In figure 7.1 it's shown the different types of images. (a) and (b) correspond to occluded pupils by eyelashes. The fit ellipse method works well on these images because the method doesn't need all the shape defined to draw an ellipse. This method uses the thresholded region to fit an ellipse in it, and if the rest of the shape is well defined the method success.

(c) and (d) images correspond to elliptical pupils. The method has no eccentricity limit due to vertical variations. Because it's possible to have an elliptical eye as seen in the figures. The (e) and (f) samples correspond to different sizes of pupils. The method has several size limits because some statistics about the pupil size were done.

In figure 7.2 it's shown different types of errors of the algorithm. (a) and (b) shows a threshold error. The threshold is not accurate, so the thresholded surface is not accurate. As seen in chapter 5 the method thresholds the darker surface.

(c) - (e) samples correspond to mistaken images due to specular reflections. The specular reflections are white surfaces in the eye. The specular reflections are almost white pixels. Anyway, if the specular reflections are in the pupil the segmentation is good but in those cases the white surface is in the edge of the pupil.

(f) sample show an unique mistaken image. The mistake is not in the fit ellipse method, instead of that is in the circular Hough Transform. As we said, the circular Hough Transform cast votes in the edge map to choose the best defined circle. In this particular case, the specular reflections, the eyelashes and the iris shape are making the best defined circle for Hough Transform.

In figure 7.3 it's shown some statistics about the processed pupils. A histogram of the pupil radius and an image with the position of the pupil centres, it shows an accumulation in the real position of the image.

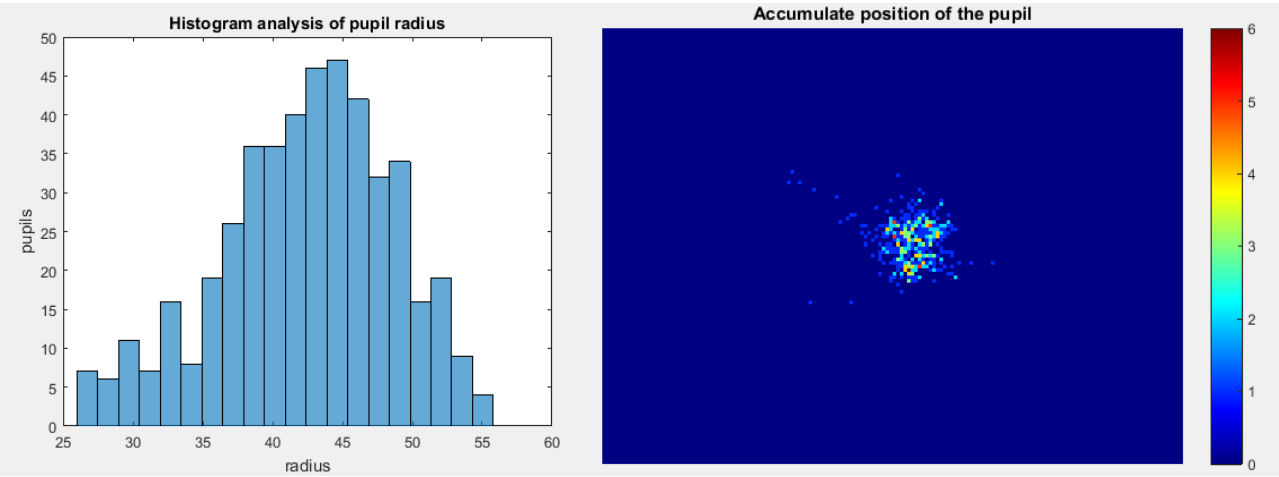

Figure 7.3: From left to right, histogram analysis of pupil radius and accumulate position of the pupil.

7.1.2 Iris Detection

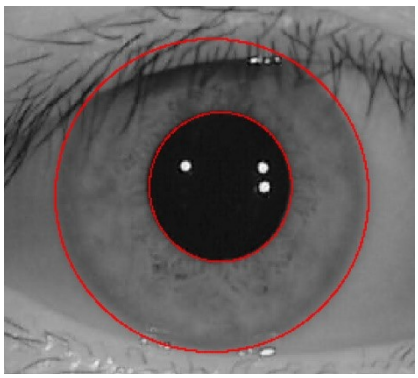

(a)

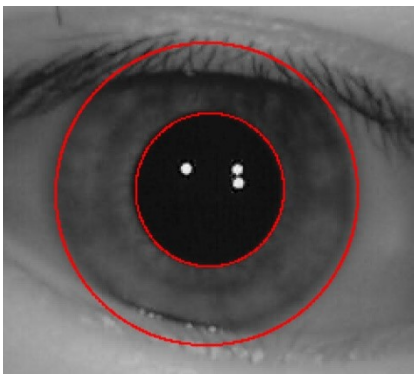

(b)

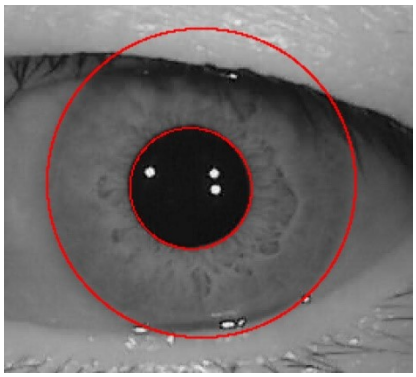

(c)

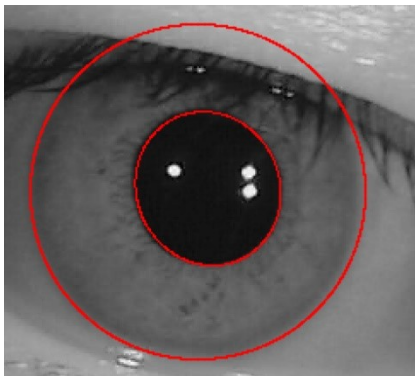

(d)

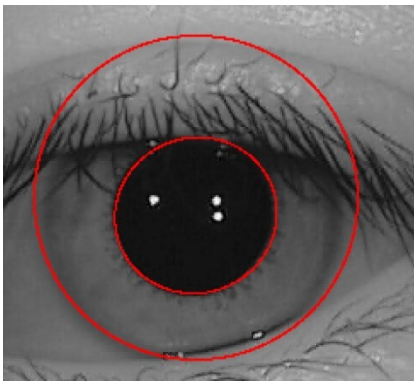

(e)

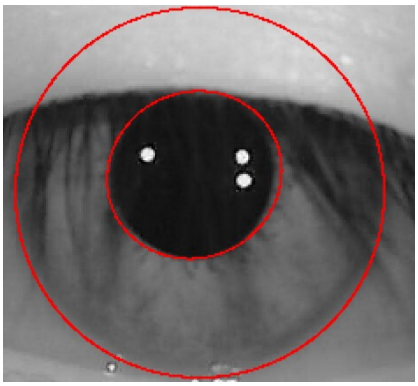

(f)

Figure 7.4: (a)-(f) illustrate the results of iris detection using the Finding radius method. The red ellipse shows the calculated result. This set of results show the well localized iris boundary.

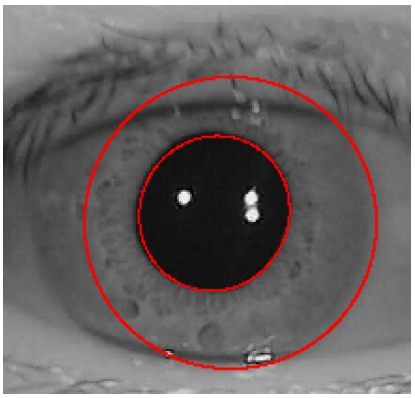

(a)

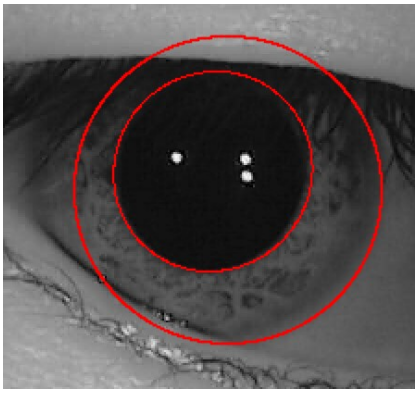

(b)

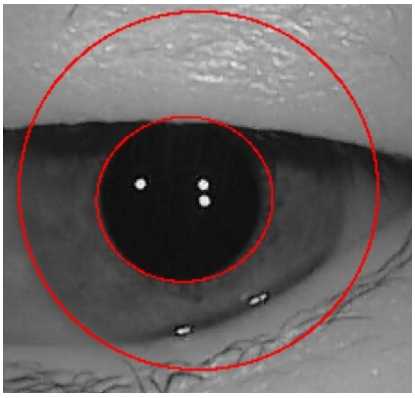

(c)

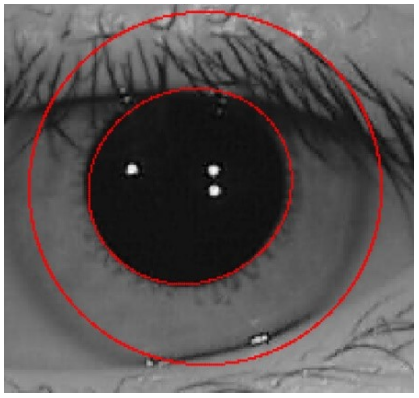

(d)

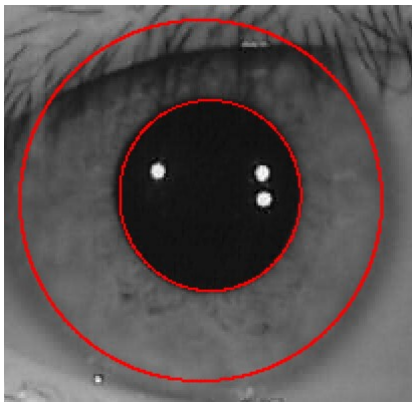

(e)

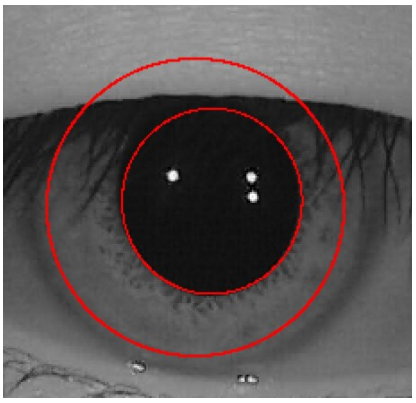

(f)

Figure 7.5: (a)-(f) illustrate the results of iris detection using the Finding radius method. The red ellipse shows the calculated result. This set of results show the bad localized iris boundary.

The performance of the proposed Finding Radius method is shown for different types of eye images in Figure 7.4. In the figure 7.5 are shown the possible errors of the algorithm.

In figure 7.4, (a) and (b) correspond to low contrast image. The contrast between the sclera and the iris pattern is low and makes it more complicate to find the edge. Anyway, the finding radius method is good with low contrast images because it compares the different possible radius and chooses the best one.

(c) and (d) images correspond to non-concentric eyes. As seen in chapter 3, off-axis orientation in eye images due to the position the subject is looking into is a factor to consider. In this case, the algorithm develops some margin in order to account these nonconcentric transformations.

(e) and (f) images show the extreme cases in which the eye is occluded by the eyelids. We can see how it occludes half of the iris pattern. The algorithm draws the iris circle with the information left. In those cases, a high contrast between sclera and iris pattern is needed.

In figure 7.5, it's shown different types of errors of the algorithm. (a) and (b) shows an error caused by the iris pattern. The iris pattern is not a completely steady surface, so that it has some abruptions. In some cases the edge contrast is greater in the iris pattern.

(c) and (d) samples correspond to extremely occluded images. The Hough Transform doesn't have enough information to make an accurate boundary. (e) and (f) images shows an edge error. In some cases, the iris pattern has a dark ring around the iris boundary. In some cases it makes two edges in the edge map used in the Hough Transform.

Below is shown statistics about the iris radius and the distance between pupil and iris centres. As seen in figure 7.6 the iris radius follows a chi distribution with centre in 90 pixels radius. In case of the distance between centres the standard deviation is bigger.

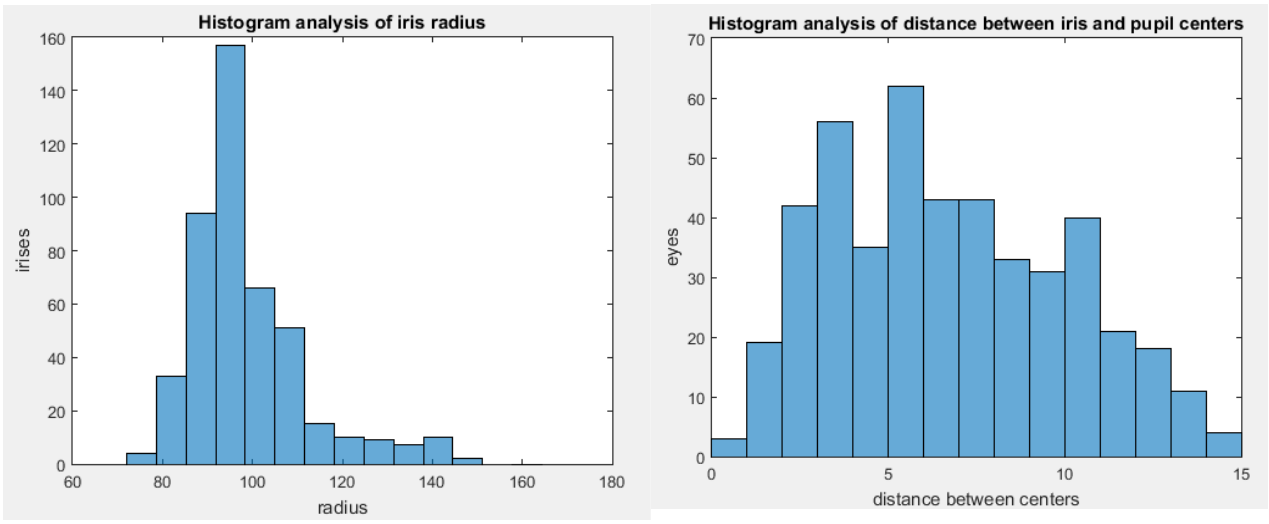

Figure 7.6: From left to right, histogram analysis of iris radius and histogram analysis between iris and pupil centres.

The proposed methods segment correctly about 87% of the database. The database is about 1200 images, and as seen in this chapter several errors are due to low contrast on the image. To have 100% accuracy in the database is needed better acquisition with better contrast.

7.2 Statistics of Iris Normalization

The iris normalization consists in changing the coordinates of the image. So, if the iris is well segmented this step is a safe procedure. Anyway, the warping method is discussed. In figure 7.7, an off-axis orientated image is shown to show how the algorithm is warping. The left area of the segmented iris is decimated and the right is interpolated. It achieves the idea of normalize the off-axis orientation.

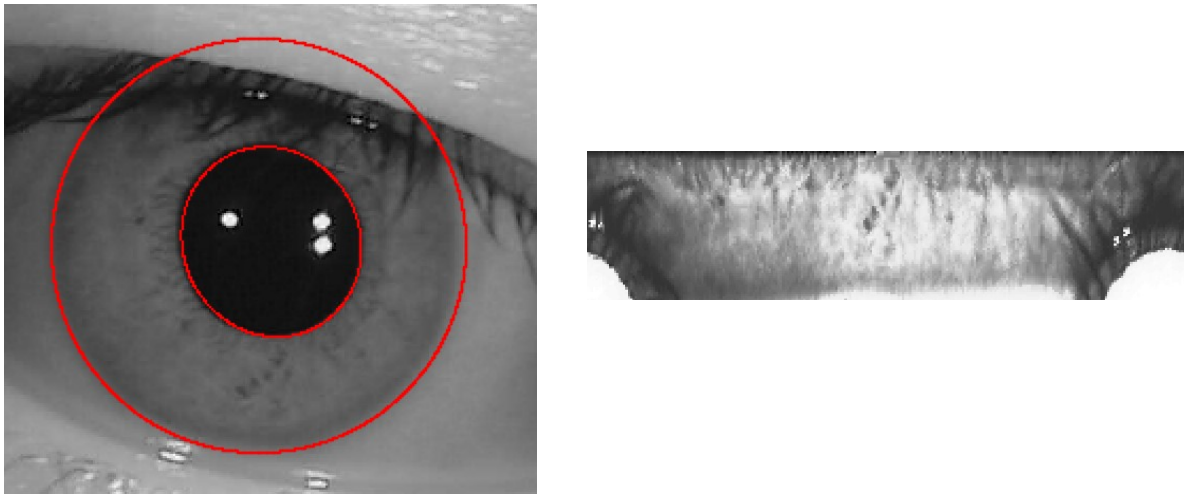

Figure 7.7: Iris Normalization of a segmented iris

7.2.1 Eliminating Eyelids

The algorithm eliminates the eyelids by thresholding the normalized iris. Considering the iris pattern as a grey surface is possible to threshold the dark and light areas. Furthermore, the occlusions are localized so it's easier to detect the eyelashes and skin. In figure 7.8, is shown some examples of the resulted iris. If the region is bigger enough, the eyelid of the centre of the image is thresholded. If the iris pattern is occluded by the eyelids the left region used to the comparison procedure would be insufficient.

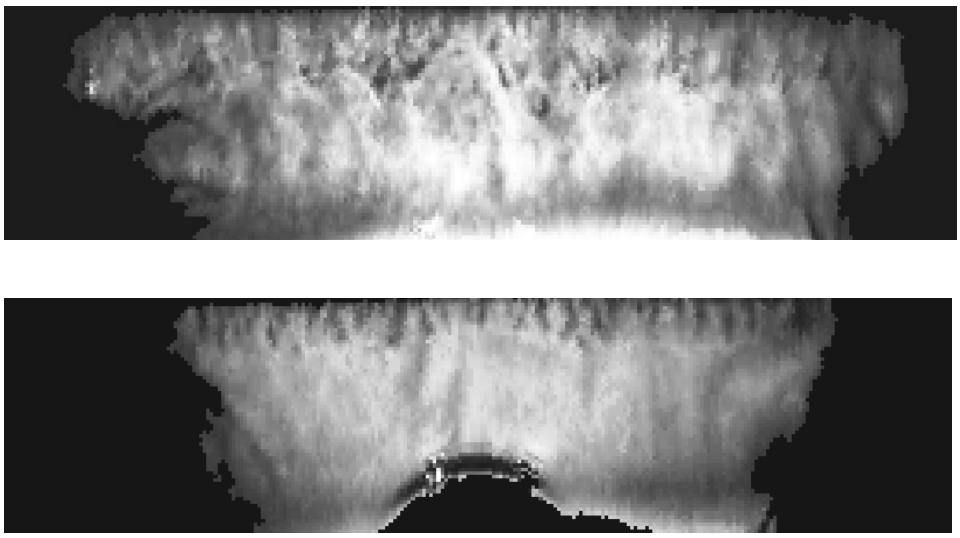

Figure 7.8: Thresholded iris patterns

7.2.2 Image Enhancement

The aim of the image enhancement is to improve the image quality. Adjusting and equalizing the histogram is a well-known procedure and improves its contrast. In figure 7.9 are shown the enhanced images of figure 7.8

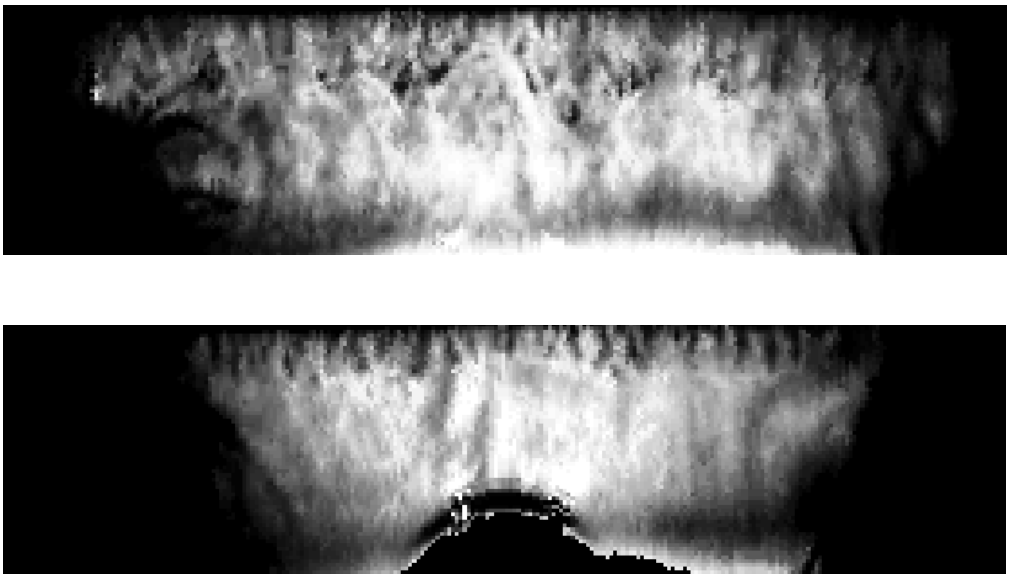

Figure 7.9: Enhanced iris patterns

7.3 Statistics of Iris Comparison

The first test was to confirm the uniqueness of iris patterns. Testing the uniqueness of iris patterns is important, since recognition relies on iris patterns from different eyes being entirely independent, with failure of a test of statistical independence resulting in a match. Uniqueness was determined by comparing templates generated from different eyes to each other, and examining the distribution of Hamming distance values produced. This distribution is known as the inter-class distribution.

According to statistical theory, the mean Hamming distance for comparisons between inter-class iris templates will be 0.5. This is because, if truly independent, the bits in each template can be thought of as being randomly set, so there is a 50% chance of being set to 0 and a 50% chance of being set to 1. Therefore, half of the bits will agree between two templates, and half will disagree, resulting in a Hamming distance of 0.5.

The chosen parameters for the Gabor Filter are the following:

- Number of scales: 1
- Minimum Wavelength: 825 pixels
- Multiplicative factor to scales: 1
- Frequency parameter selection: 1.8

Those parameters are suitable to CASIA database due to the characteristics of the samples. The frequency parameters are linked to the image size, determined by the angular resolution and radial resolution. The selected image size is (180x45) pixels, 45 of radial resolution and 180 of angular resolution.

7.3.1 Intra-class comparison results

With the CASIA database 3534 unique intraclass comparisons are done. In other words, 3534 Hamming distance values are calculated. In figure 7.10 is shown the intra-class statistics of the CASIA database. Below are some statistics:

- Mean = 0.145
- Standard deviation = 0.103
- Minimum value = 0.0201
- Maximum value = 0.6419

The minimum and maximum values are extremely far away because of the variety of the database.

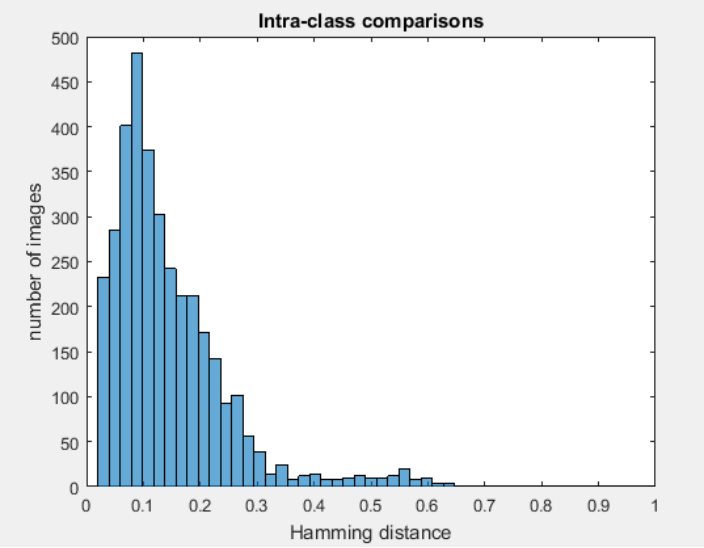

Figure 7.10: Inter-class comparisons

7.3.2 Inter-class comparison results

With the CASIA database 4031 unique intraclass comparisons are done. In other words, 4031 Hamming distance values are calculated. In figure 7.11 is shown the inter-class statistics.

- Mean = 0.440
- Standard deviation = 0.104
- Minimum value = 0.0938
- Maximum value = 0.7282

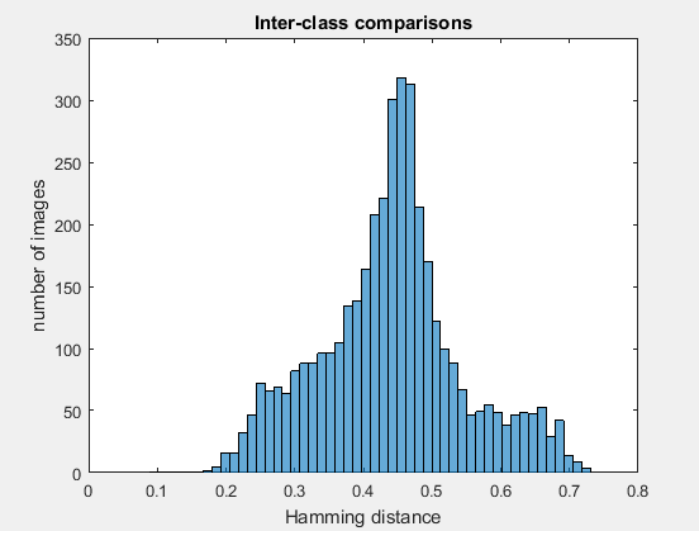

Figure 7.11: Inter-class comparisons

7.3.3 Hamming Distance threshold

In summary, the optimum encoding parameters are chosen depending on the database. To choose the Hamming distance the same procedure is used. Using the Intra-class and inter-class data we can deduce the optimal threshold for this database. The threshold separates the histograms in two parts. In the Hamming distances below the threshold, the algorithm suggests that the iris patterns are from the same person. On the contrary, the Hamming distances above the threshold era from different eyes of different persons.

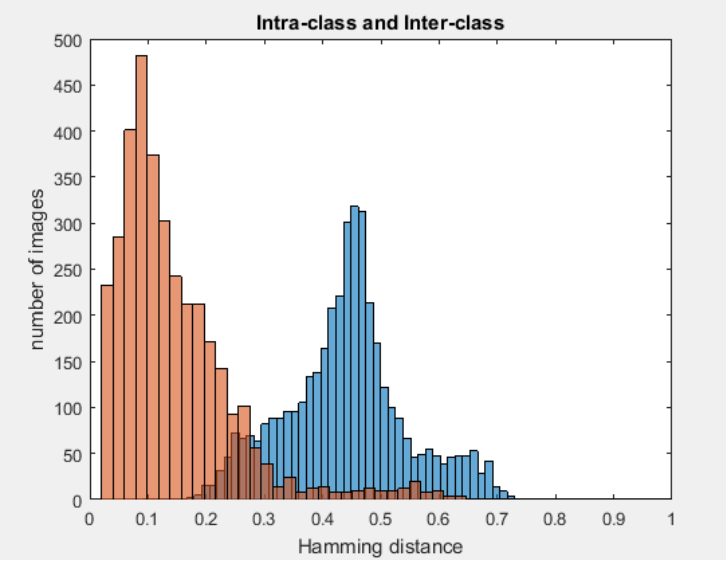

Figure 7.12: Inter-class and Intra-class comparisons

The accuracy of recognition with these distributions can be determined by calculating their false accept and false reject rates with different separation points.

Threshold	FAR (%)	FRR (%)
0.15	0.04	37.15
0.20	0.47	21.59
0.25	3.62	11.40
0.30	10.44	6.28
0.35	19.17	4.44
0.40	31.00	3.42

Table 7.13: False accept and false reject rates for CASIA database

The threshold in which the overall error is minimum is 0.25 with an overall error of 6.80%. This means the 93.2% of the dataset would be without error.

7.3.4 Performance Comparison

After seeing the results of this thesis, it would be interesting to compare the results with the state of the art algorithms. Ideally, the results should be compared to different methods working on the same databases.

Some papers works on different CASIA databases, such as CASIA v3 and CASIA v1. This work is about CASIA v2 device 1, so that the result comparisons are complicated to achieve. Anyway, some comparisons about the final results are going to be discussed. In table 7.14, some results are showed from different methods.

Database	Method	Accuracy (%)
CASIA v3	NIT Rourkela [22]	95.07
CASIA v2	Ruiz-Schulcloper [23]	96.83
CASIA v2	Proposed Method	93.2

Table 7.13: Results comparison between different methods

The results from the different methods show the environment in which the work is done. As seen, there are no methods that assure 100% accuracy for these databases. Instead of that, at least 4% of the matches are false matched.

Anyway, we can see that our method can be improved. As seen in other papers, Gabor filter parameters should be enhanced to obtain the best results for the normalized iris. For future work approaches, the parameters of the entire process can be changed. If we change the parameters, for example, of the image processing the ideal parameters of the Gabor feature changes.

In Ruiz-Schulcloper method [23], the size parameters of the ROI are changed in order to obtain the best result. It means that they used the parts of the normalized pattern that gives better results. In our case, we used the entire iris pattern to compare the iris patterns.

In NIT Rourkela method [22], the used database is CASIA v3. A priori, it seems that is a similar database but it is not. CASIA v3 database uses a different device to acquire the images. It is known that the device is one of the most important steps in iris recognition systems.

CHAPTER 8

Summary of Work

This thesis has presented an iris recognition system, which was tested using a database. Firstly, an automatic segmentation algorithm was proposed and developed, which would localise the iris region from an eye and isolate the eyelid and eyelash. Automatic segmentation was achieved through the fit ellipse method and finding radius method.

Next, the segmented iris region was normalised to eliminate dimensional inconsistencies between iris regions. This was achieved by implementing a version of Daugman's rubber sheet model, where the iris is modelled as a flexible rubber sheet. In order to fix off-axis orientations, in which the subject doesn't look into the lens of the camera a wrapping method was developed. The wrapping method normalizes the iris regardless of the position of the pupil in respect of the iris.

Finally, features of the iris were encoded by convolving the normalised iris region with 1D Log-Gabor filters and phase quantising the output in order to produce a bitwise biometric template. The Hamming distance was chosen as a matching metric, which gave a measure of how many bits disagreed between two templates. A failure of statistical independence between two templates would result in a match, that is, the two templates were deemed to have been generated from the same iris if the Hamming distance produced was lower than a set Hamming distance.

Bibliography

[1] Daugman, J. (2004). “How Iris Recognition Works”. IEEE Transactions on Circuits and Systems for Video Technology, vol. 14, no. 1,

[2] Daugman, J. (2005). “Results From 200 Billion Iris Cross-Comparisons”. Technical Report published by the University of Cambridge, no. 635.

[3] Biometric sample quality – Part 1: Framework, 2016.

[4] Information technology – Vocabulary – Part 37: Biometrics, 2015.

[5] Information technology - Vocabulary - Part 37: Biometrics, 2012.

[6] OKI IRISPASS-h. “Handheld Iris Camera and Iris Recognition Software”. <www.oki.com/iris>

[7] Trokielewicz, M. (2015). “Exploring the feasibility of iris recognition for visible spectrum iris images obtained using smartphone camera”. Biometrics Laboratory, Research and Academic Computer Network. Warsaw, Poland.

[8] OKI. “Note on CASIA-Iris V2”. <http://biometrics.idealtest.org/>. GuangZhou, China in Dec. 2004.

[9] InterNational Committee for Information Technology Standards, Biometric Sample Quality Standard Draft (Revision 4), document number M1/06-0003, February 7,2005.

[10] Information technology. Biometric sample quality. Part 1: Framework, 2009.

[11] Daugman, J. (1993). “High Confidence Visual Recognition of Persons by a Test of Statistical Independence.” IEEE Transactions on Pattern Analysis and Machine Intelligence, Vol. 15, No.11, pp.1148-1161.

[12] Arvacheh, E. (2006). “A Study of Segmentation and Normalization for Iris Recognition Systems”. University of Waterloo. Ontario, Canada.

[13] Daugman, J. (2007). “New Methods in Iris Recognition” IEEE Transactions on Systems, Man and Cybernetics – Part B: Cybernetics, Vol. 37, No 5.

[14] Masek, L. (2003). “Recognition of Human Iris Patterns for Biometric Identification” The University of Western Australia.

[15] Kazakov, T. (2011). “Iris Detection and Normalization”. Publication at: <https://www.researchgate.net/publication/216206388 >.

[16] Huo, G. (2014). “2D-Gabor Filter Design and Parameter Selection Based on Iris Recognition” Journal of Information & Computational Science 11:6. Jilin University, Jilin, China.

[17] Tai Sing Lee, (1996). “Image Representation Using 2D Gabor Wavelets” IEEE Transactions on Pattern Analysis and Machine Intelligence, Vol. 18, No 10.

[18] Cabeza, R. (2015). “Image Segmentation” Notes of the subject “Procesado Digital de Imagen”. Universidad Pública de Navarra, Pamplona, Navarra, España.

[19] Peter Kovesi, “Matlab and Octave functions for computer vision and image processing”. <http://www.peterkovesi.com/matlabfns/>

[20] Richard Brown, “fitellipse.m”. <http://www.mathworks.com/matlabcentral/fileexchange/15125-fitellipse-m>

[21] Darren Redfern and Colin Campbell. MATLAB 5 Handbook. Springer-Verlag, Boston, 1998.

[22] Dept. of Computer Science & Engineering NIT Rourkela, “Iris Biometric System”

[23] Ruiz-Schulcloper, 2013. “Progress in Pattern Recognition, Image Analysis, Computer Vision and Applications” 18th Iberoamerican Congress.